inherited from his father, and that a missense mutation (c.2303G>A [p.Arg768His]) in exon 21 were inherited from his mother (Figure 1A). The two mutations were also present in an affected elder sister (individual 2) but not present in a healthy elder brother. In individual 3, we confirmed that a nonsense mutation (c.1648C>T [p.Arg550X]) in exon 16 was inherited from her father and that a missense mutation (c.2778C>G [p.Asp926Glu]) in exon 24 was inherited from her mother (Figure 1A). The two mutations were not present in a healthy younger brother. To examine the mutational effects of c.1857-2A>C and c.1648C>T, reverse transcription PCR and sequencing with total RNA extracted from lymphoblastoid cells derived from the individuals was performed as previously described.[11] We demonstrated that the c.1857-2A>C mutation caused deletion of exon 18 from the *POLR3B* mRNA (Figures 2A–2C), resulting in an in-frame 33 amino acid deletion (p.Asn620_Lys652del) from RPC2 (Figure 1B). In addition, the mutated transcript harboring the nonsense mutation (c.1648C>T) was found to be expressed at a much lower level compared with the wild-type transcript (Figure 2D). The expression level of the mutated transcript was increased after treatment with 30 μM cycloheximide (CHX),[11] which inhibits nonsense-mediated mRNA decay (NMD), indicating that the mutant transcript underwent NMD (Figure 2D). The two missense mutations (p.Arg768His and p.Asp926Glu) found in the three individuals occurred at evolutionary conserved amino acids (Figure 1B). Among the other candidate genes in individuals 1 and 3, *MSLN* (MIM 601051), encoding mesothelin isoform 1 preproprotein that is cleaved into megakaryocyte potentiating factor and mesothelin, is a potential candidate in the family of individual 1 as its homozygous variant segregated with the phenotype; however, it is expressed in epithelial mesotheliomas, and the mutation affects less conserved amino acid (Table S3). The other candidate genes' variants did not cosegregate with the phenotype. Thus, mutations in *POLR3B* are most likely to cause HCAHC in two families.

In individual 4, in whom no *POLR3B* mutations were found, there were six candidate genes for an autosomal-recessive model. Among them, *POLR3A* (MIM 614258, GenBank accession number NM_007055.3), harboring two missense mutations, appeared to be a primary candidate because it encodes the largest subunit of Pol III (RPC1) (Figure 1A and Table S2). By Sanger sequencing, we confirmed that a missense mutation (c.2690T>A [p.Ile897Asn]) in exon 20 was inherited from his father and that another missense mutation (c.3013C>T [p.Arg1005Cys]) in exon 23 was inherited from his mother (Figure 1A). The two mutations were not present in a healthy younger sister. The two missense mutations (p.Ile897Asn and p.Arg1005Cys) occurred at relatively conserved amino acids (Figure 1B). In total, we found four mutations in *POLR3B* and two mutations in *POLR3A*. Evaluation of the missense mutations by PolyPhen-2 program showed that three mutations (p.Arg768His,

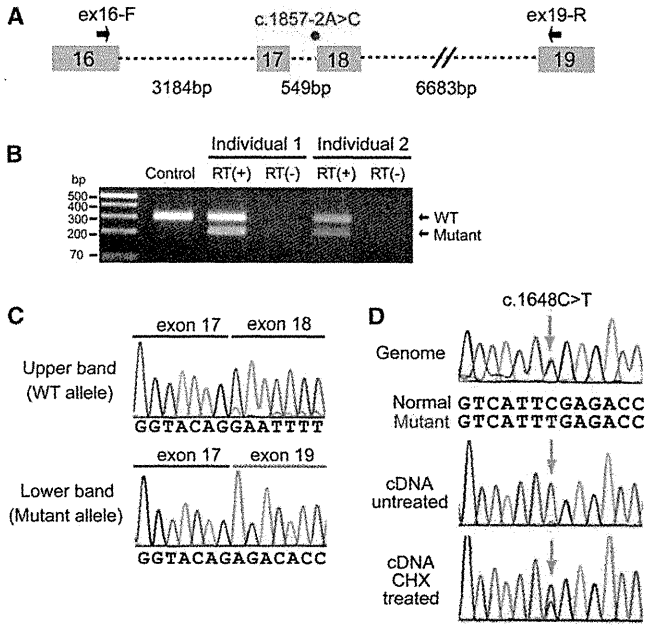

Figure 2. Effects of Splice-Site and Nonsense Mutations in *POLR3B*

(A) Schematic representation of the genomic structure of *POLR3B* from exon 16 to 19. Exons, introns, and primers are shown by boxes, dashed lines, and arrows, respectively. The mutation in intron 17 is depicted as a red dot.

(B) RT-PCR analysis of individuals 1 and 2 with c.1857-2A>C and a normal control. Two PCR products were detected from the individual's cDNA: the upper band is the wild-type (WT) transcript, and the lower band is the mutant. Only a single wild-type amplicon was detected in the control.

(C) Sequence of WT and mutant amplicons clearly showed exon 18 skipping in the mutant allele.

(D) Analysis of the c.1648C>T mutation. Sequence of PCR products amplified with genomic (upper), cDNA from untreated cells (middle), and cDNA from CHX treated cells (lower) as a template. Although untreated cells show extremely low levels of c.1648C>T mutant allele expression, cells treated to inhibit NMD show significantly increased levels of mutant allele expression.

p.Asp926Glu, and p.Ile897Asn) were probably damaging and that p.Arg1005Cys is tolerable. The c.2303G>A mutation (*POLR3B*) was found in one allele out of 540 Japanese control chromosomes. The remaining five mutations were not detected in 540 Japanese control chromosomes, indicating that the mutations are very rare in the Japanese population. Among the other candidate genes in individuals 4, *IGSF10*, a member of immunoglobulin superfamily, is a potential candidate because its variants segregated with the phenotype (Table S3); however, considering a close relationship between *POLR3A* and *POLR3B*, and the fact that *POLR3A* mutations have been recently reported in hypomyelinating leukodystrophy (see below),[12] *POLR3A* abnormality is the most plausible culprit for HCAHC in individual 4.

The structure of Pol III[13,14] and Pol II[15,16] is highly homologous, especially in the largest subunits. Thus, we extrapolated the mutations of RPC1 or RPC2 onto the structure of yeast Pol II (Protein Data Bank [PDB] accession number 3GTP)[17] (Figure 1C). RPB1 and RPB2 subunits of

yeast Pol II are homologous to RPC1 and RPC2 of Pol III, respectively. Asn620_Lys652 in RPC2 corresponds to Tyr679_Lys712 in RPB2. The deletion of Asn620_Lys652 (Tyr679_Lys712) would destroy a structural core of RPB2, leading to loss of RPB2 function. In addition, Arg768 (Arg852 in RPB2) interacts with the main-chain carbonyl group of Arg70 of the RPB12 subunit, and Asp926 (Asp1009 in RPB2) interacts with the side chain of Arg48 of the RPB10 subunit of Pol II (Figure 1D). Arg768His (Arg852His) and Asp926Glu (Asp1009Glu) substitutions are considered to disturb these subunit interactions, leading to dysfunction of the polymerase. Therefore, structural prediction suggests that the mutations in *POLR3B* (RPC2) could affect Pol III function. On the other hand, Ile897 and Arg1005 in RPC1 correspond to Val863 and Arg1036 in RPB1, respectively. Ile897 (Val863) has hydrophobic interactions with Leu170 and Pro176 of the RPB5 subunit and with Phe900 (Phe866) of the RPB1 subunit of Pol II (Figure 1E). Ile897Asn (Val863Asn) substitution is likely to disturb this interaction. Arg1005 (Arg1036) stabilizes interaction between RPB1 and RPB8 subunits (Figure 1F). The Arg1005Cys (Arg1036Cys) substitution appears to make this interaction unstable. Thus mutations in *POLR3A* are also predicted to affect Pol III function.

Clinical features of individuals with *POLR3A* or *POLR3B* mutations are presented in Table 1. MRI revealed high-intensity areas in the white matter in T2-weighted images, cerebellar atrophy, and a hypoplastic corpus callosum in all four individuals (Figure 3). Individuals 1 and 2 showed an extremely similar clinical course. They developed normally during their early infancy, i.e., walking unaided at 15 and 14 months, and uttering a few words at 12 and 13 months, respectively. After the age of 3, individual 1 presented with unstable walking and frequent stumbling and falling down, and individual 2 became poor at exercise. They both had severe myopia (corrected visual acuity of 0.7 and 0.5 at most, respectively). They graduated from elementary, junior high, and high schools with poor records, and the intelligence quotient (IQ) of individual 2 was 52 (WAIS-III). In individual 1, unstable walking was prominent at around 18 years, and he could not ride a bicycle because of ataxia; however, he could drive an automobile. Amenorrhea was noted in individual 2, and was successfully treated by hormone therapy. Individual 1 showed several signs of hypogonadism, including absence of underarm and mustache hair, thin pubic hair (Tanner II), and serum levels of testosterone, follicle stimulating hormone, and luteinizing hormone that were below normal for age 27. Neurological examination of both individuals revealed mild horizontal nystagmus, slowing of smooth-pursuit eye movement, and gaze limitation, especially in vertical gazing, hypotonia, mildly exaggerated deep-tendon reflex (patellar and Achilles tendon reflex) with negative Babinski reflex, and cerebellar signs and symptoms, including ataxic speech, wide-based ataxic gait, dysdiadochokinesis, and dysmetria. Clinical information for individual 3 has been reported previously.[6] Additional findings are as follows: slowing of smooth-pursuit eye movement, gaze limitation in vertical gazing, normal auditory brain responses (ABR), cerebral symptoms with mild spasticity, and intellectual disability (an IQ of 43 according to the WISC-III test), and no myopia but hypermetropic astigmatism. She showed no deterioration besides a mild dysphagia and walks herself to a school for the disabled. Individual 4 developed normally during his

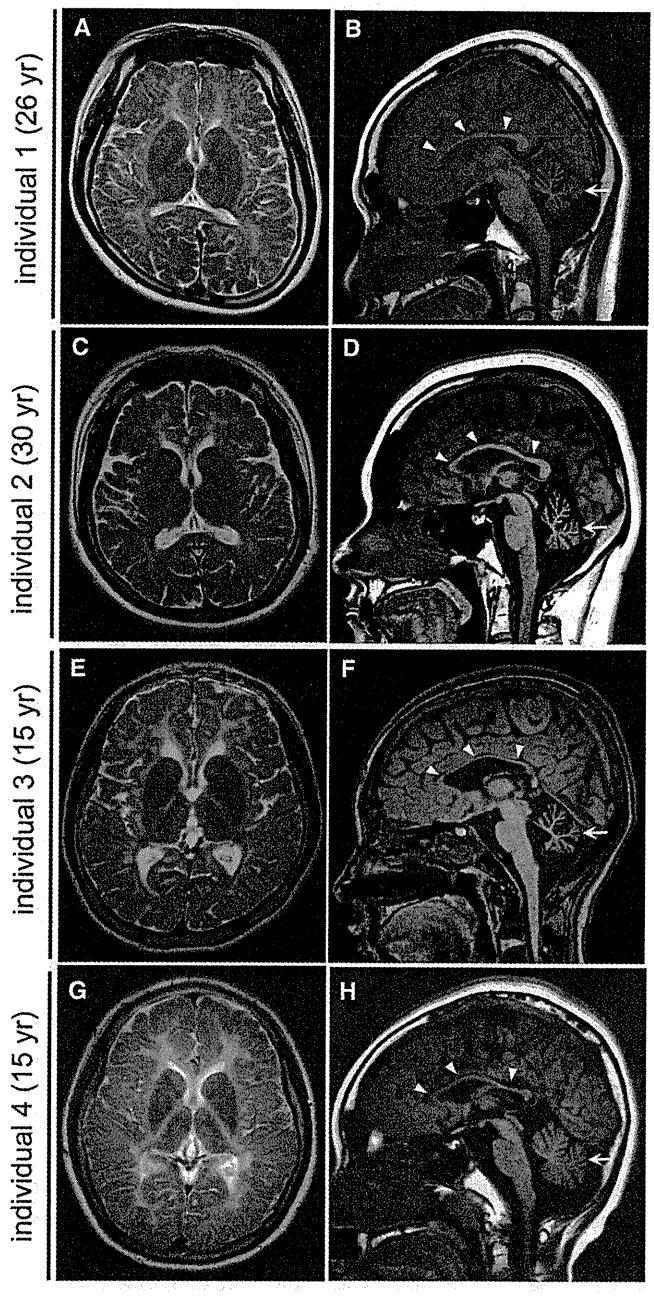

Figure 3. Brain MRI of Individuals with *POLR3B* and *POLR3A* Mutations

(A, C, E, and G) T2-weighted axial images through the basal ganglia. High-intensity areas in the white matter were observed in all individuals.

(B, D, F, and H) T1-weighted midline sagittal images. All the individuals showed hypoplastic corpus callosum (arrowheads) and atrophy of cerebellum (arrows).

early infancy, had normal head control at 3 months, was speaking a few words at 12 months, and was walking unaided at 14 months. His parents noted mild tremors around 4 years. He had normal stature, weight, and head circumference. Although he had severe myopia, his eye movement was smooth with no limitation or nystagmus. He had sensory neuronal deafness on the left side. He showed normal muscle tone and had no spasticity or rigidity. His tendon reflexes were slightly elevated with a negative Babinski reflex. Cerebellar signs were noted; expressive ataxic explosive speech, intension tremor, poor finger to nose test, dysdiadochokinesis, dysmetria, and wide-based ataxic gait. His intelligence quotient was 57 (according to the WISC-III test). His peripheral nerve conduction velocity was within the normal range and his ABR showed normal responses on the right side. He suffered motor deterioration around age 14 and became wheelchair bound.

In this study, we successfully identified compound heterozygous mutations in *POLR3A* and *POLR3B* in individuals with HCAHC. Very recently, Bernard et al.[12] reported that *POLR3A* mutations cause three overlapping leukodystrophies, including 4H syndrome, suggesting that HCAHC is, at least in part, within a wide clinical spectrum caused by *POLR3A* mutations. The p.Arg1005Cys mutation was shared between individual 9 in their report and our individual 4. All 19 individuals with *POLR3A* mutations showed progressive upper motor neuron dysfunction and cognitive regression. In addition, individual 9 showed abnormal eye movement, hypodontia, and hypogonadism. None of these features were recognized in our individual 4; these differences further support phenotypic variability of *POLR3A* mutations.[12] Given the phenotypic similarities among 4H syndrome, HCAHC, and H-ABC, there is a possibility that H-ABC is also allelic and caused by recessive mutations in either *POLR3A* or *POLR3B*.

Pol III consists of 17 subunits and is involved in the transcription of small noncoding RNAs, such as 5S ribosomal RNA (rRNA), U6 small nuclear RNA (snRNA), 7SL RNA, RNase P, RNase MRP, short interspersed nuclear elements (SINEs), and all transfer RNAs (tRNAs). Pol III-transcribed genes are classified into three types based on promoter elements and transcription factors. 5S rRNA is a solo type I gene. Type II genes include tRNA, 7SL RNA, and SINEs. Type III genes include U6 snRNA, RNase P, and RNase MRP.[18–20] The Pol III system is important for cell growth in yeast, and its transcription is tightly regulated during the cell cycle.[20] In zebrafish, *polr3b* mutant larvae that have a deletion of 41 conserved amino acids (Δ239-279) from the Rpc2 protein showed a proliferation deficit in multiple tissues, including intestine, endocrine pancreas, liver, retina and terminal branchial arches.[21] In the mutants, the expression levels of tRNA were significantly reduced, whereas the level of 5S rRNA expression was not changed, suggesting that this *polr3b* mutation can differentially affect Pol III target promoters.[21] RPC2 contributes to the catalytic activity of the polymerase and forms the active center of the polymerase together with the largest subunit, RPC1.[22] Thus, it is reasonable to consider that mutations in *POLR3A* and *POLR3B* cause overlapping phenotypes. Indeed, three individuals with *POLR3B* mutations showed diffuse cerebral hypomyelination, atrophy of the cerebellum and corpus callosum, and abnormal eye movements that overlap with *POLR3A* abnormalities.[12] Furthermore, two out of three individuals showed hypogonadism, suggesting a common pathological mechanism between *POLR3A* and *POLR3B* mutations. In the zebrafish *polr3b* mutants there were no defects of the central nervous system other than a reduced size of the retina, probably reflecting species differences; however, the reduced level of tRNA in the *polr3b* mutants raises the possibility that defects of tRNA transcription by Pol III could be a common pathological mechanism underlying *POLR3A* and *POLR3B* mutations. Supporting this idea, mutations in two genes involved in aminoacylation activity of tRNA synthetase cause defects of myelination in central nervous system: *DARS2* (MIM 610956) and *AIMP* (MIM 603605).[23,24] In addition, mutations in four genes encoding aminoacyl-tRNA synthetase cause Charcot-Marie-Tooth disease (MIM 613641, 613287, 601472, and 608323), resulting from demyelination of peripheral nerve axons: *KARS* (MIM 601421), *GARS* (MIM 600287), *YARS* (MIM 603623), and *AARS* (MIM 601065).[25–28] Thus, it is very likely that regulation of tRNA expression is essential for development and maintenance of myelination in both central and peripheral nervous systems.

An interesting clinical feature of *POLR3B* mutations is the absence of motor deterioration. All three individuals with *POLR3B* mutations could walk without support at ages 16, 27, and 30, whereas individual 3 with *POLR3A* mutations had motor deterioration around age 14. Bernard et al.[12] also reported progressive upper motor neuron dysfunction and cognitive regression in individuals with *POLR3A* mutations. Thus, there is a possibility that phenotypes caused by *POLR3A* mutations could be more severe and progressive than *POLR3B* mutant phenotypes. Identification of a greater number of cases with *POLR3B* mutations is required to confirm this hypothesis.

In conclusion, our data, together with that of a previous report,[12] demonstrate that mutations in Pol III subunits cause overlapping autosomal-recessive hypomyelinating disorders. Establishment of an animal model will facilitate our understanding of the pathophysiology of the multiple defects caused by Pol III mutations.

Supplemental Data

Supplemental Data include three tables and can be found with this article online at http://www.cell.com/AJHG/.

Acknowledgments

We would like to thank all the individuals and their families for their participation in this study. This work was supported by

research grants from the Ministry of Health, Labour, and Welfare (H.S., H.O., M.S., J.T., N. Miyake, K.I. and N. Matsumoto), the Japan Science and Technology Agency (N. Matsumoto), a Grant-in-Aid for Scientific Research on Innovative Areas (Foundation of Synapse and Neurocircuit Pathology) from the Ministry of Education, Culture, Sports, Science and Technology of Japan (N. Matsumoto), a Grant-in-Aid for Scientific Research from Japan Society for the Promotion of Science (H.O., N. Matsumoto), a Grant-in-Aid for Young Scientist from Japan Society for the Promotion of Science (H.S.). This work has been done at Advanced Medical Research Center, Yokohama City University.

Received: August 31, 2011
Revised: October 5, 2011
Accepted: October 10, 2011
Published online: October 27, 2011

Web Resources

The URLs for data presented herein are as follows:

ClustalW, http://www.genome.jp/tools/clustalw/
dbSNP, http://www.ncbi.nlm.nih.gov/projects/SNP/
Ensembl, http://uswest.ensembl.org/index.html
GenBank, http://www.ncbi.nlm.nih.gov/Genbank/
Online Mendelian Inheritance in Man, http://www.omim.org
PolyPhen-2, http://genetics.bwh.harvard.edu/pph2/
Protein Data Bank, http://www.pdb.org/pdb/home/home.do
PyMOL, http://www.pymol.org/
SeattleSeq Annotation, http://gvs.gs.washington.edu/SeattleSeq Annotation/

References

1. Schiffmann, R., and van der Knaap, M.S. (2009). Invited article: an MRI-based approach to the diagnosis of white matter disorders. Neurology *72*, 750–759.
2. Timmons, M., Tsokos, M., Asab, M.A., Seminara, S.B., Zirzow, G.C., Kaneski, C.R., Heiss, J.D., van der Knaap, M.S., Vanier, M.T., Schiffmann, R., and Wong, K. (2006). Peripheral and central hypomyelination with hypogonadotropic hypogonadism and hypodontia. Neurology *67*, 2066–2069.
3. Wolf, N.I., Harting, I., Boltshauser, E., Wiegand, G., Koch, M.J., Schmitt-Mechelke, T., Martin, E., Zschocke, J., Uhlenberg, B., Hoffmann, G.F., et al. (2005). Leukoencephalopathy with ataxia, hypodontia, and hypomyelination. Neurology *64*, 1461–1464.
4. Wolf, N.I., Harting, I., Innes, A.M., Patzer, S., Zeitler, P., Schneider, A., Wolff, A., Baier, K., Zschocke, J., Ebinger, F., et al. (2007). Ataxia, delayed dentition and hypomyelination: a novel leukoencephalopathy. Neuropediatrics *38*, 64–70.
5. van der Knaap, M.S., Naidu, S., Pouwels, P.J., Bonavita, S., van Coster, R., Lagae, L., Sperner, J., Surtees, R., Schiffmann, R., and Valk, J. (2002). New syndrome characterized by hypomyelination with atrophy of the basal ganglia and cerebellum. AJNR Am. J. Neuroradiol. *23*, 1466–1474.
6. Sasaki, M., Takanashi, J., Tada, H., Sakuma, H., Furushima, W., and Sato, N. (2009). Diffuse cerebral hypomyelination with cerebellar atrophy and hypoplasia of the corpus callosum. Brain Dev. *31*, 582–587.
7. Li, H., Ruan, J., and Durbin, R. (2008). Mapping short DNA sequencing reads and calling variants using mapping quality scores. Genome Res. *18*, 1851–1858.
8. Doi, H., Yoshida, K., Yasuda, T., Fukuda, M., Fukuda, Y., Morita, H., Ikeda, S., Kato, R., Tsurusaki, Y., Miyake, N., et al. (2011). Exome sequencing reveals a homozygous *SYT14* mutation in adult-onset, autosomal-recessive spinocerebellar ataxia with psychomotor retardation. Am. J. Hum. Genet. *89*, 320–327.
9. Pierce, S.B., Walsh, T., Chisholm, K.M., Lee, M.K., Thornton, A.M., Fiumara, A., Opitz, J.M., Levy-Lahad, E., Klevit, R.E., and King, M.C. (2010). Mutations in the DBP-deficiency protein HSD17B4 cause ovarian dysgenesis, hearing loss, and ataxia of Perrault Syndrome. Am. J. Hum. Genet. *87*, 282–288.
10. Gilissen, C., Arts, H.H., Hoischen, A., Spruijt, L., Mans, D.A., Arts, P., van Lier, B., Steehouwer, M., van Reeuwijk, J., Kant, S.G., et al. (2010). Exome sequencing identifies *WDR35* variants involved in Sensenbrenner syndrome. Am. J. Hum. Genet. *87*, 418–423.
11. Saitsu, H., Kato, M., Okada, I., Orii, K.E., Higuchi, T., Hoshino, H., Kubota, M., Arai, H., Tagawa, T., Kimura, S., et al. (2010). *STXBP1* mutations in early infantile epileptic encephalopathy with suppression-burst pattern. Epilepsia *51*, 2397–2405.
12. Bernard, G., Chouery, E., Putorti, M.L., Tetreault, M., Takanohashi, A., Carosso, G., Clement, I., Boespflug-Tanguy, O., Rodriguez, D., Delague, V., et al. (2011). Mutations of *POLR3A* Encoding a Catalytic Subunit of RNA Polymerase Pol III Cause a Recessive Hypomyelinating Leukodystrophy. Am. J. Hum. Genet. *89*, 415–423.
13. Jasiak, A.J., Armache, K.J., Martens, B., Jansen, R.P., and Cramer, P. (2006). Structural biology of RNA polymerase III: subcomplex C17/25 X-ray structure and 11 subunit enzyme model. Mol. Cell *23*, 71–81.
14. Fernández-Tornero, C., Böttcher, B., Riva, M., Carles, C., Steuerwald, U., Ruigrok, R.W., Sentenac, A., Müller, C.W., and Schoehn, G. (2007). Insights into transcription initiation and termination from the electron microscopy structure of yeast RNA polymerase III. Mol. Cell *25*, 813–823.
15. Cramer, P., Bushnell, D.A., and Kornberg, R.D. (2001). Structural basis of transcription: RNA polymerase II at 2.8 angstrom resolution. Science *292*, 1863–1876.
16. Gnatt, A.L., Cramer, P., Fu, J., Bushnell, D.A., and Kornberg, R.D. (2001). Structural basis of transcription: an RNA polymerase II elongation complex at 3.3 A resolution. Science *292*, 1876–1882.
17. Wang, D., Bushnell, D.A., Huang, X., Westover, K.D., Levitt, M., and Kornberg, R.D. (2009). Structural basis of transcription: backtracked RNA polymerase II at 3.4 angstrom resolution. Science *324*, 1203–1206.
18. Oler, A.J., Alla, R.K., Roberts, D.N., Wong, A., Hollenhorst, P.C., Chandler, K.J., Cassiday, P.A., Nelson, C.A., Hagedorn, C.H., Graves, B.J., and Cairns, B.R. (2010). Human RNA polymerase III transcriptomes and relationships to Pol II promoter chromatin and enhancer-binding factors. Nat. Struct. Mol. Biol. *17*, 620–628.
19. Dieci, G., Fiorino, G., Castelnuovo, M., Teichmann, M., and Pagano, A. (2007). The expanding RNA polymerase III transcriptome. Trends Genet. *23*, 614–622.
20. Dumay-Odelot, H., Durrieu-Gaillard, S., Da Silva, D., Roeder, R.G., and Teichmann, M. (2010). Cell growth- and differentiation-dependent regulation of RNA polymerase III transcription. Cell Cycle *9*, 3687–3699.

21. Yee, N.S., Gong, W., Huang, Y., Lorent, K., Dolan, A.C., Maraia, R.J., and Pack, M. (2007). Mutation of RNA Pol III subunit *rpc2/polr3b* Leads to Deficiency of Subunit Rpc11 and disrupts zebrafish digestive development. PLoS Biol. *5*, e312.
22. Werner, M., Thuriaux, P., and Soutourina, J. (2009). Structure-function analysis of RNA polymerases I and III. Curr. Opin. Struct. Biol. *19*, 740–745.
23. Scheper, G.C., van der Klok, T., van Andel, R.J., van Berkel, C.G., Sissler, M., Smet, J., Muravina, T.I., Serkov, S.V., Uziel, G., Bugiani, M., et al. (2007). Mitochondrial aspartyl-tRNA synthetase deficiency causes leukoencephalopathy with brain stem and spinal cord involvement and lactate elevation. Nat. Genet. *39*, 534–539.
24. Feinstein, M., Markus, B., Noyman, I., Shalev, H., Flusser, H., Shelef, I., Liani-Leibson, K., Shorer, Z., Cohen, I., Khateeb, S., et al. (2010). Pelizaeus-Merzbacher-like disease caused by AIMP1/p43 homozygous mutation. Am. J. Hum. Genet. *87*, 820–828.
25. Latour, P., Thauvin-Robinet, C., Baudelet-Méry, C., Soichot, P., Cusin, V., Faivre, L., Locatelli, M.C., Mayençon, M., Sarcey, A., Broussolle, E., et al. (2010). A major determinant for binding and aminoacylation of tRNA(Ala) in cytoplasmic Alanyl-tRNA synthetase is mutated in dominant axonal Charcot-Marie-Tooth disease. Am. J. Hum. Genet. *86*, 77–82.
26. McLaughlin, H.M., Sakaguchi, R., Liu, C., Igarashi, T., Pehlivan, D., Chu, K., Iyer, R., Cruz, P., Cherukuri, P.F., Hansen, N.F., et al. (2010). Compound heterozygosity for loss-of-function lysyl-tRNA synthetase mutations in a patient with peripheral neuropathy. Am. J. Hum. Genet. *87*, 560–566.
27. Antonellis, A., Ellsworth, R.E., Sambuughin, N., Puls, I., Abel, A., Lee-Lin, S.Q., Jordanova, A., Kremensky, I., Christodoulou, K., Middleton, L.T., et al. (2003). Glycyl tRNA synthetase mutations in Charcot-Marie-Tooth disease type 2D and distal spinal muscular atrophy type V. Am. J. Hum. Genet. *72*, 1293–1299.
28. Jordanova, A., Irobi, J., Thomas, F.P., Van Dijck, P., Meerschaert, K., Dewil, M., Dierick, I., Jacobs, A., De Vriendt, E., Guergueltcheva, V., et al. (2006). Disrupted function and axonal distribution of mutant tyrosyl-tRNA synthetase in dominant intermediate Charcot-Marie-Tooth neuropathy. Nat. Genet. *38*, 197–202.

RESEARCH ARTICLE

AMERICAN JOURNAL OF medical genetics PART A

Submicroscopic Deletion in 7q31 Encompassing *CADPS2* and *TSPAN12* in a Child With Autism Spectrum Disorder and PHPV

Nobuhiko Okamoto,[1]* Yoshikazu Hatsukawa,[2] Keiko Shimojima,[3] and Toshiyuki Yamamoto[3]

[1]Department of Medical Genetics, Osaka Medical Center and Research Institute for Maternal and Child Health, Osaka, Japan

[2]Department of Ophthalmology, Osaka Medical Center and Research Institute for Maternal and Child Health, Osaka, Japan

[3]Institute for Integrated Medical Sciences, Tokyo Women's Medical University, Tokyo, Japan

Received 23 August 2010; Accepted 9 March 2011

We performed array comparative genomic hybridization utilizing a whole genome oligonucleotide microarray in a patient with the autism spectrum disorders (ASDs) and persistent hyperplastic primary vitreous (PHPV). Submicroscopic deletions in 7q31 encompassing *CADPS2* (Ca^{2+}-dependent activator protein for secretion 2) and *TSPAN12* (one of the members of the tetraspanin superfamily) were confirmed. The *CADPS2* plays important roles in the release of neurotrophin-3 and brain-derived neurotrophic factor. Mutations in *TSPAN12* are a relatively frequent cause of familial exudative vitreoretinopathy. We speculate that haploinsufficiency of *CADPS2* and *TSPAN12* contributes to ASDs and PHPV, respectively.

Key words: *CADPS2*; *TSPAN12*; autism; PHPV; CGH

How to Cite this Article:
Okamoto N, Hatsukawa Y, Shimojima K, Yamamoto T. 2011. Submicroscopic deletion in 7q31 encompassing *CADPS2* and *TSPAN12* in a child with autism spectrum disorder and PHPV.
Am J Med Genet Part A 155:1568–1573.

INTRODUCTION

Autism spectrum disorders (ASDs OMIM %209850) are complex neurodevelopmental conditions characterized by social communication disabilities, no or delayed language development, and stereotyped and repetitive behaviors. A number of studies have confirmed that genetic factors play an important role in ASDs.

About 10% of ASDs are associated with a Mendelian syndrome (e.g., fragile X syndrome, tuberous sclerosis and Timothy syndrome). Cytogenetic approaches revealed a high frequency of large chromosomal abnormalities (3–7% of patients), including the most frequently observed maternal 15q11-13 duplication (1–3% of patients). Association studies and mutation analysis of candidate genes have implicated the synaptic genes *NLGN3*(Neuroligin3 OMIM*300336), *NLGN4* (OMIM*300427) [Jamain et al., 2003], *SHANK3* (OMIM*606230)[Durand et al., 2007; Moessner et al., 2007], *NRXN1*(Neurexin1 MIM+600565) [Kim et al., 2008], *SHANK2* (OMIM*603290) [Berkel et al., 2010], and *CNTNAP2* (MIM*604569) [Alarcón et al., 2008; Arking et al., 2008] in ASDs. There is increasing evidence that the *SHANK3-NLGN4-NRNX1* postsynaptic density genes play important roles in the pathogenesis of ASDs.

Recently, on association between de novo copy number variation (CNV) and ASDs was revealed. Sebat et al. [2007] performed comparative genomic hybridization (CGH) on the genomic DNA from ASD patients and unaffected subjects to detect de novo CNV. As a result, they identified CNV in 12 out of 118 (10%) patients with sporadic ASD and confirmed de novo CNV were significantly associated with ASDs. Marshall et al. [2008] performed a genome-wide search for structural abnormalities in 427 unrelated ASD patients using SNP microarray analysis and karyotyping. De novo CNV were found in approximately 7% and approximately 2% of idiopathic families with one ASD child, or two or more ASD siblings, respectively. These authors discovered a CNV at 16p11.2 with an approximate frequency of 1%. Glessner et al. [2009] reported the results from a whole-genome CNV study of many European ASD patients and controls and found several new susceptibility genes encoding neuronal cell-adhesion molecules, including *NLGN1* and *ASTN2*, and genes involved in the ubiquitin pathways, including *UBE3A*, *PARK2*, *RFWD2*, and *FBXO40*. The investigators suggested that two gene networks, neuronal cell-

Grant sponsor: Ministry of Health, Labour and Welfare of Japan.
*Correspondence to:
Nobuhiko Okamoto, Department of Medical Genetics, Osaka Medical Center and Research Institute for Maternal and Child Health, 840 Murodo-cho, Izumi, Osaka 594-1101, Japan. E-mail: okamoto@osaka.email.ne.jp
Published online 27 May 2011 in Wiley Online Library (wileyonlinelibrary.com).
DOI 10.1002/ajmg.a.34028

adhesion and ubiquitin degradation, that are expressed within the central nervous system contribute to the genetic susceptibility of ASDs.

The International Molecular Genetic Study of Autism Consortium [1998] previously identified linkage loci on chromosomes 7 and 2, which were termed AUTS1 and AUTS5, respectively. Further genetic studies have provided evidence for AUTS1 being located on chromosome 7q [The International Molecular Genetic Study of Autism Consortium 2001]. Screening for mutations in six genes mapping to 7q, *CUTL1*, *SRPK2*, *SYPL*, *LAMB1*, *NRCAM*, and *PTPRZ1* in 48 unrelated individuals with autism led to the identification of several new coding variants in the *CUTL1*, *LAMB1*, and *PTPRZ1*genes [Bonora et al., 2005].

The human Ca^{2+}-dependent activator protein for secretion 2 (*CADPS2*: OMIM*609978) is also located on chromosome 7q31, which is within the AUTS1 locus [Cisternas et al., 2003]. It is a member of the CAPS/CADPS protein family that regulates the secretion of dense-core vesicles, which are abundant in the parallel fiber terminals of granule cells in the cerebellum and play important roles in the release of neurotrophin-3 (NT-3) and brain-derived neurotrophic factor (BDNF) [Sadakata et al., 2007a,b,c]. BDNF is indispensable for brain development and function, including the formation of synapses. Cisternas et al. [2003] studied *CADPS2* mutations in 90 unrelated autistic individuals, but identified no disease-specific variants. However, Sadakata et al. [2007a] reported that an aberrant, alternatively spliced *CADPS2* mRNA that lacks exon 3 (*CADPS2* Delta exon3) is detected in some patients with ASD.

Persistent hyperplastic primary vitreous (PHPV) is an ocular malformation caused by the presence of a retrolental fibrovascular membrane and the persistence of the posterior portion of the tunica vasculosa lentis and the hyaloid artery. It is often accompanied by microphthalmos, cataracts, and glaucoma. *NDP* (OMIM *300658, X-linked) and *FZD4* (OMIM *604579, dominant) were found to be mutated in unilateral and bilateral PHPV [Shastry, 2009]. These genes also cause Norrie disease and familial exudative vitreoretinopathy (FEVR), which share some clinical features with PHPV. FEVR is a genetically heterogeneous retinal disorder characterized by abnormal vascularization of the peripheral retina, which is often accompanied by retinal detachment. Mutations in the genes encoding *LRP5* (OMIM *603506, dominant and recessive) also cause FEVR. Junge et al. [2009] showed that *Tetraspanin12* (*Tspan12*) is expressed in the retinal vasculature, and loss of *Tspan12* phenocopies defects are seen in Fzd4, *Lrp5*, and *Norrin* mutant mice. *TSPAN12* is one of the members of the tetraspanin superfamily, characterized by the presence of four transmembrane domains. It constitutes large membrane complexes with other molecules. Nikopoulos et al. [2010] applied next-generation sequencing and found a mutation in *TSPAN12* (MIM*613168). Poulter et al. [2010] described seven mutations that were identified in a cohort of 70 FEVR patients without mutations in three known genes. Mutations in *TSPAN12*, which is at 7q31, are a relatively frequent cause of FEVR.

We performed array comparative genomic hybridization (array-CGH) utilizing a 44K whole genome oligonucleotide microarray in a patient with the ASDs and PHPV. Submicroscopic deletions in 7q31 encompassing *CADPS2* and *TSPAN12* were confirmed. We speculate that haploinsufficiency of *CADPS2* and *TSPAN12* contributes to ASD and PHPV, respectively.

CLINICAL REPORT

The patient, a 3-year-old boy, was born to nonconsanguineous healthy Japanese parents. His family history was unremarkable. He was born at 40 weeks' of gestation, his birth weight was 3,100 g, and his birth length was 50.0 cm. After birth, congenital nystagmus was noted, and he did not pursuit objects. An ophthalmological examination revealed bilateral PHPV. Cataract, glaucoma, and FEVR were not present. His gross motor development was normal, and his verbal development was delayed.

At 3 years of age, he came to our hospital for evaluation because of developmental delay. On examination dysmorphic features included a round face, low-set ears, broad eyebrows, apparent hypertelorism, blepharophimosis, hypoplastic alae nasi, a long philtrum, and a small mouth. His visual acuity was low, but he could perform daily activities with some support. In addition, impairment of social interaction, poor social skills, and strict adherence to routine behaviors were noted. He showed stereotypic movements and hyperactivity in his day care room. He was diagnosed as having an ASD according to the DSM-VI criteria. His DQ was 76 according to standard Japanese method. At 3 years and 8 months of age, his height, weight, and head circumference were 88.6 cm (−2.4 SD), 11.7 kg (−1.8 SD), and 46.8 cm (−2.4 S.D), respectively.

The results of routine laboratory tests were unremarkable. G-banded karyotype analysis revealed the following karyotype: 46,XY,inv(4)(p14;q21). Electroencephalography (EEG) showed occipital epileptic discharges. He was free from epileptic seizures.

Ultrasound evaluation revealed echogenic bands in the posterior segments of both globes. Magnetic resonance brain imaging also showed bilateral fibrous intraocular tissue (Fig. 1). However, no specific findings were found in the CNS including the cerebellum.

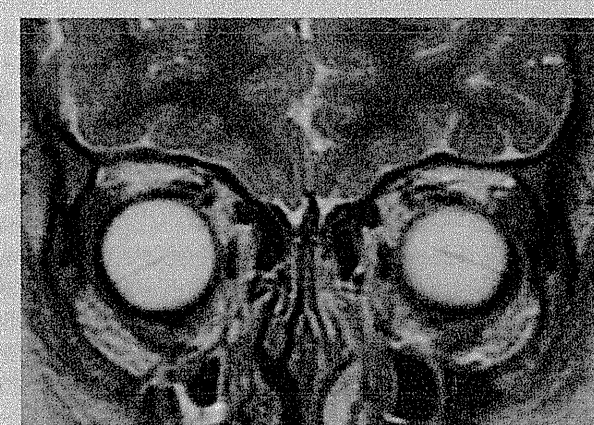

FIG. 1. MR coronal image, T2-weighted. Magnetic resonance imaging also showed fibrous intraocular tissue in the eye. [Color figure can be seen in the online version of this article, available at http://onlinelibrary.wiley.com/journal/10.1002/(ISSN)1552-4833]

MATERIALS AND METHODS

After obtaining informed consent based on a permission approved by the institution's ethical committee, peripheral blood samples were obtained from the patient and his parents. Genomic DNA was extracted using the QIAquick DNA extraction kit (QIAgen, Valencia, CA).

Array-CGH analysis was performed using the Human Genome CGH Microarray 44K (Agilent Technologies, Santa Clara, CA), as described previously [Shimojima et al., 2009].

Metaphase nuclei were prepared from peripheral blood lymphocytes using standard methods and were used for FISH analysis with human BAC clones selected from the UCSC genome browser (http://www.genome.ucsc.edu), as described elsewhere [Shimojima et al., 2009]. Physical positions refer to the March 2006 human reference sequence (NCBI Build 36.1).

RESULTS

Using array-CGH analysis, genomic copy number loss was identified in the 7q31.31 region (Fig. 2). The deletion was 5.4 Mb in size and included *CADPS2* and *TSPAN12*, but not *FOXP2*. There were no copy number changes in chromosome 4. FISH analyses confirmed the above deletion (Fig. 3). There were no deletions in either parent indicating de novo occurrence.

DISCUSSION

We described a patient with an ASD and PHPV who demonstrated submicroscopic deletion in chromosome 7q31.31. The deletion resides in the AUTS1 locus on chromosome 7q. The deleted region contained about 20 genes including *CADPS2* and *TSPAN12*. Little data are available about the association of other genes with developmental and ophthalmological disorders. We posit that haploinsufficiency of *CADPS2* and *TSPAN12* contributes to ASDs and PHPV, respectively.

Our patient fulfilled the DSM-VI criteria for an ASD. Poor eye contact, impairment of social interaction, poor social skills with strict adherence to routine, stereotypic movements, and hyperactivity were noted. However, his intellectual disability was mild. Ataxic movement was not observed.

There have been several reports of small deletions on chromosome 7q. Lennon et al. [2007] reported a young male with moderate intellectual disability, dysmorphic features, and language delay who had a deletion in the 7q31.1-7q31.31 region, which included the *FOXP2* gene. The patient demonstrated language impairment, including developmental verbal dyspraxia, but did not meet the criteria for autism. Cukier et al. [2009] reported a chromosomal inversion spanning the region from approximately 7q22.1 to 7q31 in autistic siblings. They suggested that an autism susceptibility gene is located in the chromosome 7q22–31 region. Dauwerse et al.

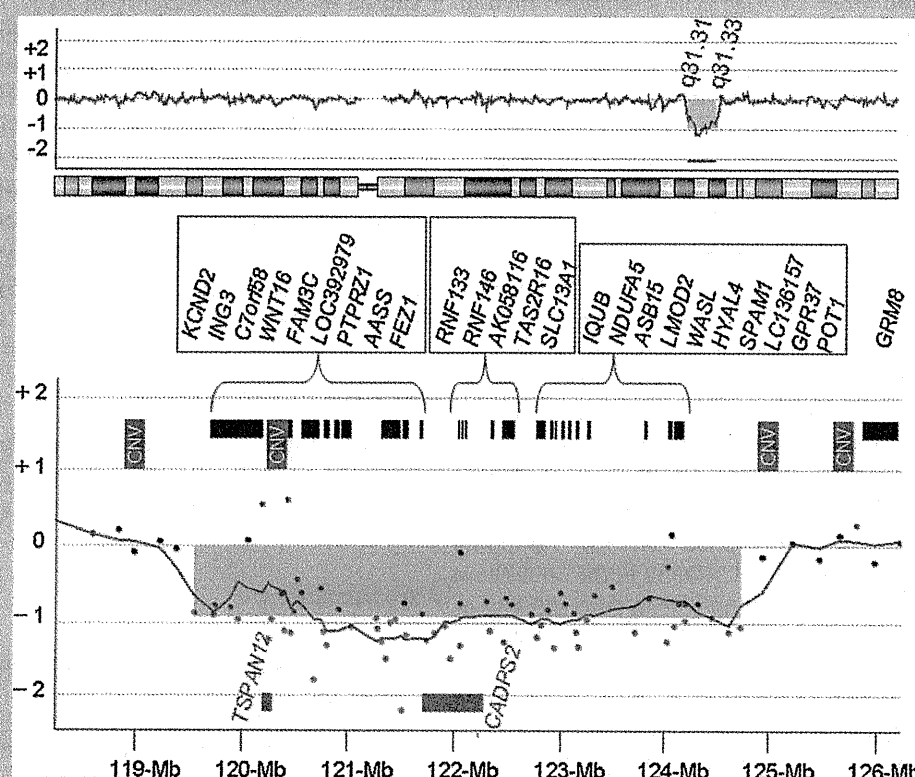

FIG. 2. Array-CGH of the patient. Loss of the genomic copy numbers was identified in the region of 7q31.31. The deletion size was 5.4 Mb and included *CADPS2* and *TSPAN12*.

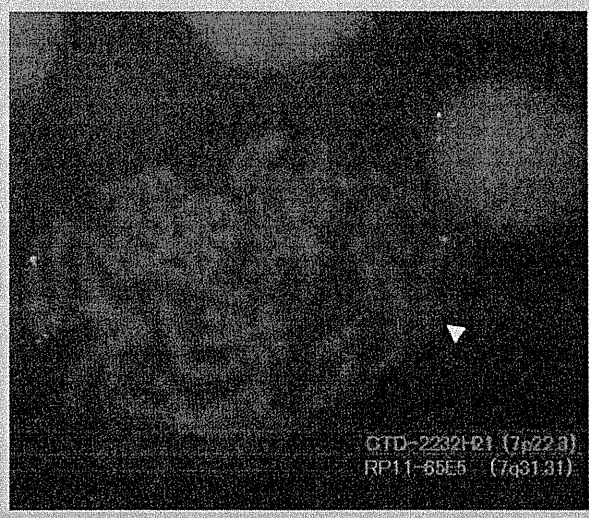

FIG. 3. FISH analyses of the patient. Arrow head indicates the deletion at 7q31.31.

[2010] characterized a de novo complex rearrangement of the long arm of chromosome 7 in a female patient with moderate mental retardation, anxiety disorder, and autistic features and suggested that disruption of the *C7orf58* gene contributed to the anxiety disorder, and autistic features of their patient. The *C7orf58* gene was also deleted in our patient. However, there have been no basic studies on the association of the *C7orf58* gene and brain function. Further studies are necessary on the role of the *C7orf58* gene.

Sadakata et al. [2007b] studied the behavior of *Cadps2−/−* mice. They showed impaired social interaction, hyperactivity, decreased exploratory behavior, and/or increased anxiety in a novel environment and deficits in intrinsic sleep–wake regulation and circadian rhythmicity. In addition, maternal neglect of newborns was a striking feature. They identified that *Cadps2−/−* mice show deficient release of NT-3 and BDNF. Cerebellar development was impaired in the mice. Sadakata et al. [2007a] found an aberrant alternatively spliced *CADPS2* mRNA that lacks exon 3 in some autistic patients. Exon 3 was shown to encode the dynactin 1-binding domain and affect axonal CADPS2 protein distribution. Exon 3-skipped CADPS2 protein possesses almost normal BDNF releasing activity but is not properly transported into the axons of neocortical or cerebellar neurons. However, Eran et al. [2009] observed no difference in prevalence of exon 3 skipping between ASDs and control samples. They concluded that exon 3 skipping represents a normal, minor isoform of CADPS2 in the cerebellum and is likely not a mechanism underlying autism susceptibility or pathogenesis. Our result may reinforce the evidence that *CADPS2* is associated with ASDs.

Cisternas et al. [2003] studied *CADPS2* gene mutations in 90 unrelated autistic individuals. However, they identified no disease-specific variants. Their results indicate that *CADPS2* mutations are not a major cause of ASDs. However, although small deletions of *CADPS2* as found in the present patient, might be rare, they support the idea that *CADPS2* abnormalities are associated with autism susceptibility.

Nikopoulos et al. [2010] reported two missense mutations in five of 11 FEVR families, indicating that mutations in *TSPAN12* are a relatively frequent cause of FEVR. Both residues are completely conserved throughout vertebrate evolution. These authors suggested that both haploinsufficiency and a dominant-negative effect of the mutant TSPAN12 on the wild-type protein should be considered as underlying disease mechanisms. Poulter et al. [2010] described mutations in the *TSPAN12* gene in FEVR patients and suggested that haploinsufficiency of *TSPAN12* causes FEVR because at least four of the seven mutations are predicted to lead to transcripts with premature-termination codons that are likely to be targeted by nonsense-mediated decay.

Recently, the Norrin/Frizzled4 signaling pathway that acts on the on the surface of developing endothelial cells and controls retinal vascular development is highlighted [Ye et al., 2010]. This pathway is composed of Norrin, its transmembrane receptor, Frizzled4, coreceptor, Lrp5, and an auxiliary membrane protein, Tspan12. The resulting signal controls a transcriptional program that regulates endothelial growth and maturation. PHPV and FEVR are associated with their pathogenesis. Our findings indicate that haploinsufficiency of *TSPAN12* is a plausible causative mechanism for PHPV. It will be interesting to study *TSPAN12* abnormalities in PHPV without *NDP* and *FZD4* mutations.

Singh et al. [2006] reported a voltage-gated potassium channel gene mutation in a temporal lobe epilepsy patient, namely a Kv4.2 truncation mutation lacking the last 44 amino acids in the carboxyl terminal. Kv4.2 channel is encoded by the *KCND2* gene. We suggest that the epileptic discharges on EEG reflect neuronal excitability caused by haploinsufficiency of *KCND2*.

Shen et al. [2010] suggested that using chromosomal microarray analysis to test for submicroscopic genomic deletions and duplications should be considered as part of the initial diagnostic evaluation of patients with ASDs. Miller et al. [2010] suggested that the use of chromosomal microarray is recommended as the first-tier cytogenetic diagnostic test for patients with unexplained developmental delay/intellectual disability, ASDs, or multiple congenital anomalies. In patients with ASDs and other anomalies, chromosomal microarray may be the useful method to clarify the underlying defect.

ACKNOWLEDGMENTS

We thank the patient's family for their cooperation. This study was supported by Health and Labour Research Grants from the Ministry of Health, Labour and Welfare of Japan.

REFERENCES

Alarcón M, Abrahams BS, Stone JL, Duvall JA, Perederiy JV, Bomar JM, Sebat J, Wigler M, Martin CL, Ledbetter DH, Nelson SF, Cantor RM, Geschwind DH. 2008. Linkage, association, and gene-expression analyses identify CNTNAP2 as an autism-susceptibility gene. Am J Hum Genet 82:150–159.

Arking DE, Cutler DJ, Brune CW, Teslovich TM, West K, Ikeda M, Rea A, Guy M, Lin S, Cook EH, Chakravarti A. 2008. A common genetic variant in the neurexin superfamily member CNTNAP2 increases familial risk of autism. Am J Hum Genet 82:160–164.

Berkel S, Marshall CR, Weiss B, Howe J, Roeth R, Moog U, Endris V, Roberts W, Szatmari P, Pinto D, Bonin M, Riess A, Engels H, Sprengel R, Scherer SW, Rappold GA. 2010. Mutations in the SHANK2 synaptic scaffolding gene in autism spectrum disorder and mental retardation. Nat Genet 42:489–491.

Bonora E, Lamb JA, Barnby G, Sykes N, Moberly T, Beyer KS, Klauck SM, Poustka F, Bacchelli E, Blasi F, Maestrini E, Battaglia A, Haracopos D, Pedersen L, Isager T, Eriksen G, Viskum B, Sorensen EU, Brondum-Nielsen K, Cotterill R, Engeland H, Jonge M, Kemner C, Steggehuis K, Scherpenisse M, Rutter M, Bolton PF, Parr JR, Poustka A, Bailey AJ, Monaco AP, International Molecular Genetic Study of Austism Consortium. 2005. Mutation screening and association analysis of six candidate genes for autism on chromosome 7q. Eur J Hum Genet 13:198–207.

Cisternas FA, Vincent JB, Scherer SW, Ray PN. 2003. Cloning and characterization of human CADPS and CADPS2, new members of the Ca^{2+}-dependent activator for secretion protein family. Genomics 81: 279–291.

Cukier HN, Skaar DA, Rayner-Evans MY, Konidari I, Whitehead PL, Jaworski JM, Cuccaro ML, Pericak-Vance MA, Gilbert JR. 2009. Identification of chromosome 7 inversion breakpoints in an autistic family narrows candidate region for autism susceptibility. Autism Res 2: 258–266.

Dauwerse JG, Ruivenkamp CA, Hansson K, Marijnissen GM, Peters DJ, Breuning MH, Hilhorst-Hofstee Y. 2010. A complex chromosome 7q rearrangement identified in a patient with mental retardation, anxiety disorder, and autistic features. Am J Med Genet Part A 152A:427–433.

Durand CM, Betancur C, Boeckers TM, Bockmann J, Chaste P, Fauchereau F, Nygren G, Rastam M, Gillberg IC, Anckarsäter H, Sponheim E, Goubran-Botros H, Delorme R, Chabane N, Mouren-Simeoni MC, de Mas P, Bieth E, Rogé B, Héron D, Burglen L, Gillberg C, Leboyer M, Bourgeron T. 2007. Mutations in the gene encoding the synaptic scaffolding protein SHANK3 are associated with autism spectrum disorders. Nat Genet 39:25–27.

Eran A, Graham KR, Vatalaro K, McCarthy J, Collins C, Peters H, Brewster SJ, Hanson E, Hundley R, Rappaport L, Holm IA, Kohane IS, Kunkel LM. 2009. Comment on "Autistic-like phenotypes in Cadps2-knockout mice and aberrant CADPS2 splicing in autistic patients". J Clin Invest 119: 679–680.

Glessner JT, Wang K, Cai G, Korvatska O, Kim CE, Wood S, Zhang H, Estes A, Brune CW, Bradfield JP, Imielinski M, Frackelton EC, Reichert J, Crawford EL, Munson J, Sleiman PM, Chiavacci R, Annaiah K, Thomas K, Hou C, Glaberson W, Flory J, Otieno F, Garris M, Soorya L, Klei L, Piven J, Meyer KJ, Anagnostou E, Sakurai T, Game RM, Rudd DS, Zurawiecki D, McDougle CJ, Davis LK, Miller J, Posey DJ, Michaels S, Kolevzon A, Silverman JM, Bernier R, Levy SE, Schultz RT, Dawson G, Owley T, McMahon WM, Wassink TH, Sweeney JA, Nurnberger JI, Coon H, Sutcliffe JS, Minshew NJ, Grant SF, Bucan M, Cook EH, Buxbaum JD, Devlin B, Schellenberg GD, Hakonarson H. 2009. Autism genome-wide copy number variation reveals ubiquitin and neuronal genes. Nature 459:569–573.

International Molecular Genetic Study of Autism Consortium. 1998. A full genome screen for autism with evidence for linkage to a region on chromosome 7q. Hum Mol Genet 7:571–578.

International Molecular Genetic Study of Autism Consortium (IMGSAC). 2001. Further characterization of the autism susceptibility locus AUTS1 on chromosome 7q. Hum Mol Genet 10:973–982.

Jamain S, Quach H, Betancur C, Råstam M, Colineaux C, Gillberg IC, Soderstrom H, Giros B, Leboyer M, Gillberg C, Bourgeron T. Paris Autism Research International Sibpair Study. 2003. Mutations of the X-linked genes encoding neuroligins NLGN3 and NLGN4 are associated with autism. Nat Genet 34:27–29.

Junge HJ, Yang S, Burton JB, Paes K, Shu X, French DM, Costa M, Rice DS, Ye W. 2009. TSPAN12 regulates retinal vascular development by promoting Norrin- but not Wnt-induced FZD4/beta-catenin signaling. Cell 139:299–311.

Kim HG, Kishikawa S, Higgins AW, Seong IS, Donovan DJ, Shen Y, Lally E, Weiss LA, Najm J, Kutsche K, Descartes M, Holt L, Braddock S, Troxell R, Kaplan L, Volkmar F, Klin A, Tsatsanis K, Harris DJ, Noens I, Pauls DL, Daly MJ, MacDonald ME, Morton CC, Quade BJ, Gusella JF. 2008. Disruption of neurexin 1 associated with autism spectrum disorder. Am J Hum Genet 82:199–207.

Lennon PA, Cooper ML, Peiffer DA, Gunderson KL, Patel A, Peters S, Cheung SW, Bacino CA. 2007. Deletion of 7q31.1 supports involvement of FOXP2 in language impairment: Clinical report and review. Am J Med Genet A 143A:791–798.

Marshall CR, Noor A, Vincent JB, Lionel AC, Feuk L, Skaug J, Shago M, Moessner R, Pinto D, Ren Y, Thiruvahindrapduram B, Fiebig A, Schreiber S, Friedman J, Ketelaars CE, Vos YJ, Ficicioglu C, Kirkpatrick S, Nicolson R, Sloman L, Summers A, Gibbons CA, Teebi A, Chitayat D, Weksberg R, Thompson A, Vardy C, Crosbie V, Luscombe S, Baatjes R, Zwaigenbaum L, Roberts W, Fernandez B, Szatmari P, Scherer SW. 2008. Structural variation of chromosomes in autism spectrum disorder. Am J Hum Genet 82:477–488.

Miller DT, Adam MP, Aradhya S, Biesecker LG, Brothman AR, Carter NP, Church DM, Crolla JA, Eichler EE, Epstein CJ, Faucett WA, Feuk L, Friedman JM, Hamosh A, Jackson L, Kaminsky EB, Kok K, Krantz ID, Kuhn RM, Lee C, Ostell JM, Rosenberg C, Scherer SW, Spinner NB, Stavropoulos DJ, Tepperberg JH, Thorland EC, Vermeesch JR, Waggoner DJ, Watson MS, Martin CL, Ledbetter DH. 2010. Consensus statement: Chromosomal microarray is a first-tier clinical diagnostic test for individuals with developmental disabilities or congenital anomalies. Am J Hum Genet 86:749–764.

Moessner R, Marshall CR, Sutcliffe JS, Skaug J, Pinto D, Vincent J, Zwaigenbaum L, Fernandez B, Roberts W, Szatmari P, Scherer SW. 2007. Contribution of SHANK3 mutations to autism spectrum disorder. Am J Hum Genet 81:1289–1297.

Nikopoulos K, Gilissen C, Hoischen A, van Nouhuys CE, Boonstra FN, Blokland EA, Arts P, Wieskamp N, Strom TM, Ayuso C, Tilanus MA, Bouwhuis S, Mukhopadhyay A, Scheffer H, Hoefsloot LH, Veltman JA, Cremers FP, Collin RW. 2010. Next-generation sequencing of a 40 Mb linkage interval reveals TSPAN12 mutations in patients with familial exudative vitreoretinopathy. Am J Hum Genet 86:240–247.

Poulter JA, Ali M, Gilmour DF, Rice A, Kondo H, Hayashi K, Mackey DA, Kearns LS, Ruddle JB, Craig JE, Pierce EA, Downey LM, Mohamed MD, Markham AF, Inglehearn CF, Toomes C. 2010. Mutations in TSPAN12 cause autosomal-dominant familial exudative vitreoretinopathy. Am J Hum Genet 86:248–253.

Sadakata T, Washida M, Iwayama Y, Shoji S, Sato Y, Ohkura T, Katoh-Semba R, Nakajima M, Sekine Y, Tanaka M, Nakamura K, Iwata Y, Tsuchiya KJ, Mori N, Detera-Wadleigh SD, Ichikawa H, Itohara S, Yoshikawa T, Furuichi T. 2007a. Autistic-like phenotypes in Cadps2-knockout mice and aberrant CADPS2 splicing in autistic patients. J Clin Invest 117:931–943.

Sadakata T, Kakegawa W, Mizoguchi A, Washida M, Katoh-Semba R, Shutoh F, Okamoto T, Nakashima H, Kimura K, Tanaka M, Sekine Y, Itohara S, Yuzaki M, Nagao S, Furuichi T. 2007b. Impaired cerebellar development and function in mice lacking CAPS2, a protein involved in neurotrophin release. J Neurosci 27:2472–2482.

Sadakata T, Washida M, Furuichi T. 2007c. Alternative splicing variations in mouse CAP S2: Differential expression and functional properties of splicing variants. BMC Neurosci 8:25.

Sebat J, Lakshmi B, Malhotra D, Troge J, Lese-Martin C, Walsh T, Yamrom B, Yoon S, Krasnitz A, Kendall J, Leotta A, Pai D, Zhang R, Lee YH, Hicks

J, Spence SJ, Lee AT, Puura K, Lehtimäki T, Ledbetter D, Gregersen PK, Bregman J, Sutcliffe JS, Jobanputra V, Chung W, Warburton D, King MC, Skuse D, Geschwind DH, Gilliam TC, Ye K, Wigler M. 2007. Strong association of de novo copy number mutations with autism. Science 316:445–449.

Shastry BS. 2009. Persistent hyperplastic primary vitreous: Congenital malformation of the eye. Clin Experiment Ophthalmol 37:884–890.

Shen Y, Dies KA, Holm IA, Bridgemohan C, Sobeih MM, Caronna EB, Miller KJ, Frazier JA, Silverstein I, Picker J, Weissman L, Raffalli P, Jeste S, Demmer LA, Peters HK, Brewster SJ, Kowalczyk SJ, Rosen-Sheidley B, McGowan C, Duda AW III, Lincoln SA, Lowe KR, Schonwald A, Robbins M, Hisama F, Wolff R, Becker R, Nasir R, Urion DK, Milunsky JM, Rappaport L, Gusella JF, Walsh CA, Wu BL, Miller DT. Autism Consortium Clinical Genetics/DNA Diagnostics Collaboration. 2010. Clinical genetic testing for patients with autism spectrum disorders. Pediatrics 125:e727–e735.

Shimojima K, Páez MT, Kurosawa K, Yamamoto T. 2009. Proximal interstitial 1p36 deletion syndrome: The most proximal 3.5-Mb microdeletion identified on a dysmorphic and mentally retarded patient with inv(3)(p14.1q26.2). Brain Development 31:629–633.

Singh B, Ogiwara I, Kaneda M, Tokonami N, Mazaki E, Baba K, Matsuda K, Inoue Y, Yamakawa K. 2006. A Kv4.2 truncation mutation in a patient with temporal lobe epilepsy. Neurobiol Dis 24:245–253.

Ye X, Wang Y, Nathans J. 2010. The Norrin/Frizzled4 signaling pathway in retinal vascular development and disease. Trends Mol Med 16:417–425.

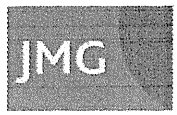

Reduced expression by *SETBP1* haploinsufficiency causes developmental and expressive language delay indicating a phenotype distinct from Schinzel –Giedion syndrome

Isabel Filges, Keiko Shimojima, Nobuhiko Okamoto, et al.

J Med Genet 2011 48: 117-122 originally published online October 30, 2010
doi: 10.1136/jmg.2010.084582

Reduced expression by *SETBP1* haploinsufficiency causes developmental and expressive language delay indicating a phenotype distinct from Schinzel–Giedion syndrome

Isabel Filges,[1] Keiko Shimojima,[2] Nobuhiko Okamoto,[3] Benno Röthlisberger,[4] Peter Weber,[5] Andreas R Huber,[4] Tsutomu Nishizawa,[6] Alexandre N Datta,[5] Peter Miny,[1] Toshiyuki Yamamoto[2]

► Additional figure and table are published online only. To view these files please visit the journal online (http://jmg.bmj.com).

[1]Division of Medical Genetics, University Children's Hospital and Department of Biomedicine, Basel, Switzerland
[2]Tokyo Women's Medical University Institute for Integrated Medical Sciences, Tokyo, Japan
[3]Osaka Medical Center and Research Institute for Maternal and Child health, Osaka, Japan
[4]Center of Laboratory Medicine, Cantonal Hospital, Aarau, Switzerland
[5]Division of Neuropediatrics and Developmental Medicine, University Children's Hospital, Basel, Switzerland
[6]Division of Virology, Department of Infectious and Immunity, Jichi Medical University School of Medicine, Shimotsuke, Japan

Correspondence to
Dr T Yamamoto, Tokyo Women's Medical University Institute for Integrated Medical Sciences, 8-1 Kawada-cho, Shinjuku-ward, Tokyo 162-8666, Japan; toshiyuki.yamamoto@twmu.ac.jp

Received 28 August 2010
Accepted 13 September 2010
Published Online First 30 October 2010

ABSTRACT

Background Mutations of the SET binding protein 1 gene (*SETBP1*) on 18q12.3 have recently been reported to cause Schinzel–Giedion syndrome (SGS). As rare 18q interstitial deletions affecting multiple genes including *SETBP1* correlate with a milder phenotype, including minor physical anomalies and developmental and expressive speech delay, mutations in *SETBP1* are thought to result in a gain-of-function or a dominant-negative effect. However, the consequence of the *SETBP1* loss-of-function has not yet been well described.

Methods Microarray-based comparative genomic hybridisation (aCGH) analyses were performed to identify genetic causes for developmental and expressive speech delay in two patients. SETBP1 expression in fibroblasts obtained from one of the patients was analysed by real-time RT-PCR and western blotting. A cohort study to identify nucleotide changes in *SETBP1* was performed in 142 Japanese patients with developmental delay.

Results aCGH analyses identified submicroscopic deletions of less than 1 Mb exclusively containing *SETBP1*. Both patients show global developmental, expressive language delay and minor facial anomalies. Decreased expression of SETBP1 was identified in the patient's skin fibroblasts. No pathogenic mutation of *SETBP1* was identified in the cohort study.

Conclusion SETBP1 expression was reduced in a patient with *SETBP1* haploinsufficiency, indicating that the *SETBP1* deletion phenotype is allele dose sensitive. In correlation with the exclusive deletion of *SETBP1*, this study delimits a milder phenotype distinct from SGS overlapping with the previously described phenotype of del(18)(q12.2q21.1) syndrome including global developmental, expressive language delay and distinctive facial features. These findings support the hypothesis that mutations in *SETBP1* causing SGS may have a gain-of-function or a dominant-negative effect, whereas haploinsufficiency or loss-of-function mutations in *SETBP1* cause a milder phenotype.

Mutations in the SET binding protein 1 gene (*SETBP1*) have recently been shown to cause Schinzel–Giedion syndrome (SGS, MIM #269150).[1] Whole-exome sequencing for four patients with SGS identified nucleotide alterations in the conserved region of *SETBP1*. Further analyses by standard Sanger sequencing for nine patients with SGS were performed, and eight of the nine patients showed *SETBP1* mutations. All five identified mutations were missense mutations, rather than nonsense mutations or truncations. As previously reported, rare chromosomal deletions in 18q including *SETBP1* correlate with a milder phenotype, and the severe SGS phenotype was proposed to be the consequence of a gain-of-function or dominant-negative effect of the mutations. However, the exact function of the gene is not known, and the consequences of an exclusive *SETBP1* loss-of-function or haploinsufficiency are not well described.

We identified de novo heterozygous microdeletions containing exclusively *SETBP1* in two patients with developmental, expressive language delay and distinctive facial features. The phenotypes are milder and differ significantly from the severe clinical appearance of SGS. Genotype–phenotype correlations of *SETBP1* haploinsufficiency are demonstrated in this study and discussed.

PATIENTS AND METHODS

Patients

After informed consent based on permission from the ethics committee of the institutions or individual written consent had been obtained, peripheral blood samples were taken from patients with developmental delay of unidentified aetiology to investigate potential genomic copy number aberrations.

Patients' reports

Patient 1 (DECIPHER #TWM253969) is a 7-year old boy, the second child of non-consanguineous parents (https://decipher.sanger.ac.uk/). His 10-year-old sister is healthy and normally developed. He was born with a birth weight of 2504 g (3–10th centile), length of 47 cm (10–25th centile), and occipitofrontal circumference (OFC) of 33.5 cm (=50th centile). At the time of his birth, his father and mother were 34 and 40 years old, respectively. His development was moderately delayed with crawling at 1 year, free walking at 2 years, and the first word at 5 years. He suffered febrile seizures several times, but EEG and brain MRI showed no abnormal findings. At 7 years, his height was 115 cm (25–50th centile), weight was 15.0 kg (<3rd centile), and OFC was 49.3 cm (3–10th centile). He showed distinctive facial features with an inverted triangle face, prominent forehead, ptosis with periorbital fullness, epicanthus and

pointed chin (figure 1A). He can walk by himself and can speak only a few words. The Kyoto developmental scale measured his developmental quotient as 40, which indicated moderate developmental delay. Visual acuity examination showed a refractive error of +8D in both eyes, indicating hyperopia. Previously performed conventional chromosomal analysis showed a normal male karyotype of 46,XY.

Patient 2, the 3rd child of non-consanguineous healthy parents, was born at 38 weeks by caesarean section for breech presentation after an uneventful pregnancy. In the neonatal period, the boy was hypotonic, sleepy and passive and rarely cried. He showed significantly delayed motor development, with sitting at 14 months and walking at 2 years, as well as delayed pincer grip. Initially, a discrete hemiparesis of the left part of his body manifested only while running with a slight spastic posture of his left hand and gait asymmetry suggested a perinatal or prenatal stroke. Cerebral MRI at the age of 4 years was normal except an unspecific T2 hyperintense infratentorial lesion in the right cranial paramedian cerebellum. The patient still exhibits coordination deficits in fine motoricity. His growth parameters are in the normal range (75th–90th centile), and OFC is within the 10th–25th centile. Hearing was found to be normal. Interestingly, the boy has not developed any expressive speech at all to date, whereas receptive language abilities are intact. He actively communicates using gestures illustrating his demands and ideas, but well understands his interlocutor, permitting a bidirectional exchange. He exhibits kind and social behaviour but at the same time a restless search for interactive communication. He has difficulty concentrating and has no sense of danger or pain. Facial dysmorphisms include frontal upsweep, a lighter blond hair corona in the front, hypertelorism, ptosis of eyelids predominantly on the left, periorbital fullness, straight and sparse eyebrows, flat nasal bridge, short nose, thin upper lip, short fingers and broad distal phalanges (figure 1B–D). No major malformations have been found. Microcytic hypochrome anaemia remains unexplained; the search for HbH inclusion bodies which would indicate X-linked α-thalassaemia/mental retardation syndrome was negative.

Microarray-based comparative genomic hybridisation (aCGH)

aCGH analyses were performed using the Human Genome CGH Microarray 44K (Agilent Technologies, Santa Clara, California, USA) and the whole genome tiling NimbleGen CGH array (Human CGH 2.1M WG-T v2.0; NimbleGen; Roche NimbleGen Inc, Madison, Wisconsin, USA) for patient 1 and patient 2, respectively, according to the manufacturer's protocols.

Fluorescence in situ hybridisation

Identified aberrations were confirmed by fluorescence in situ hybridisation (FISH) using locus-specific BAC clones as probes. In patient 1, two clones, CTD-3236P11 on 18q12.3 (chr18:40 779 351–40 864 576) as a target and RP11-105C15 on 18p11.31 (chr18:5 910 725–60 63 460) as a marker, were selected from the UCSC genome browser (http://www.genome.ucsc.edu). In patient 2, the locus-specific probe RP11-24L5 (BlueGnome, Cambridge, UK) in the region 18q12.3 (chr18:40 588 784–40 776 858) was used on metaphase spreads. Physical positions refer to the March 2006 human reference sequence (NCBI Build 36.1).

Expression analysis of SETBP1

Total RNAs were extracted from cultured skin fibroblasts from patient 1 and the control individual using the ISOGEN RNA extraction kit (Wako, Osaka, Japan), reverse-transcribed to complementary DNA (cDNA) using the SuperScript VILO cDNA Synthesis Kit (Life Technologies, Carlsbad, California, USA) according to the manufacturer's instructions, then used as templates for real-time PCR using Power SYBR Green PCR master mix (Life Technologies). Primers for SETBP1 mRNA were designed in the coding region (SETBP1 nt374F; 5′-GTCCA CCTGAGATCAAGATC-3′ and SETBP1 nt663R; 5′-GTCCATGT GGTTCTGGCTGC-3′). Beta actin primers (5′-GGCACCCAGCA CAATGAAGATC-3′ and 5′-AAGTCATAGTCCGCCTAGAAGC-3′)

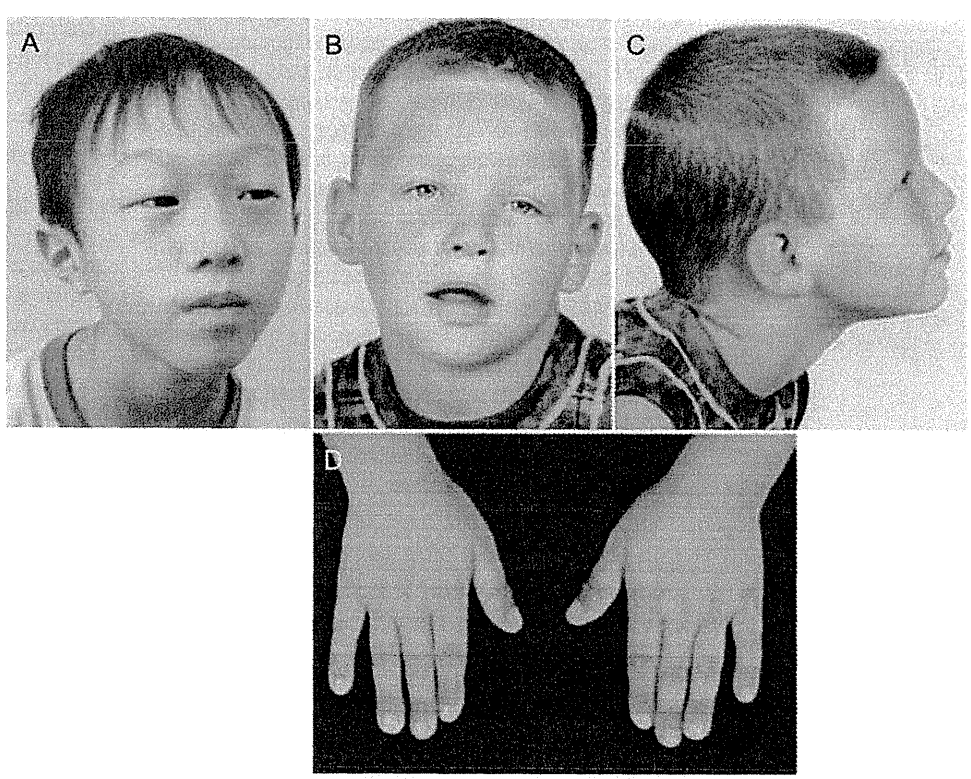

Figure 1 Phenotypes of the patients. (A) Patient 1; (B,C) frontal and lateral views of patient 2; (D) both hands of patient 2.

J Med Genet 2011;**48**:117–122. doi:10.1136/jmg.2010.084582

118

were used for the internal control. Real-time PCR amplifications were performed in three independent replicates on an ABI7500 (Life Technologies), and the data were evaluated by the Delta Delta Ct method.[2] The SETBP1 expression ratio (patient versus normal control) was calculated in each of the three examinations.

Concentrations of SETBP1 in the cell lysates of skin fibroblasts from patient 1 and the control were also analysed by western blotting using the SETBP1 MaxPab mouse polyclonal antibody (B01), catalogue number H00026040-B01 (Abnova, Taipei City, Taiwan) as described previously.[3]

Cohort study of *SETBP1*

A total of 142 Japanese patients with developmental delay, without genomic copy number aberrations as determined by aCGH, participated in the cohort study.[4] *SETBP1* sequences were analysed by the standard PCR-direct sequencing method. The primers used for PCR and the big-dye sequencing reaction (Life Technologies) were designed using Primer3 (http://primer3.sourceforge.net/) (supplemental online table 1). When we identified nucleotide changes in samples for which parental samples were available, trio analyses were performed to check whether the changes were de novo or familial. The nucleotide sequences of *SETBP1*, in which nucleotide alterations were found in the cohort study, were compared with homologues in species including *Callithrix jacchus*, *Gorilla gorilla*, *Macaca mulatta*, *Pan troglodytes*, *Pongo pygmaeus*, *Tarsius syrichta* and *Tupaia belangeri*, which were identified using Gene Tree (http://www.ensembl.org). DNA samples from 70 Japanese volunteers were used for the control cohort of normal Japanese.

RESULTS

Cytogenetic analyses

In patient 1, aCGH analysis revealed an aberration in the contiguous 11 probes at 18q12.3 with the mean $\log_2$ ratio of −1.02306 (figure 2A). This indicated a 986 kb loss of genomic copy number at 18q12.3; molecular karyotyping was determined as arr chr18q12.3q12.3 (40 282 934–41 269 199)x1. The deletion exclusively contained *SETBP1* and was confirmed by FISH analysis showing only one signal from the targeted probes (supplemental online figure S1). FISH analysis using the same probes showed no abnormality in either parent, indicating a de novo deletion (data not shown).

In patient 2, aCGH showed an 850 kb deletion within the chromosomal region 18q12.3 (chr18:40 233 803–41 088 224) (figure 2B). The deletion was confirmed by FISH, and both parents were found to be normal by conventional chromosome analysis and FISH analysis with the same locus-specific probe, indicating a de novo occurrence (data not shown). The only referenced gene within the deleted region was *SETBP1*. The two neighbouring genes, *BC051727* and *AK123972*, were non-coding. *TSLC14A2* (NM_007163) encodes a renal tubular urea transporter of the solute carrier family 14, not related to the phenotype of the patient.

Expression of SETBP1

In comparison with the normal control, SETBP1 RNA expression in the skin fibroblasts derived from patient 1 was reduced to 0.53, 0.60 and 0.41 (mean 0.51), and the lower SETBP1

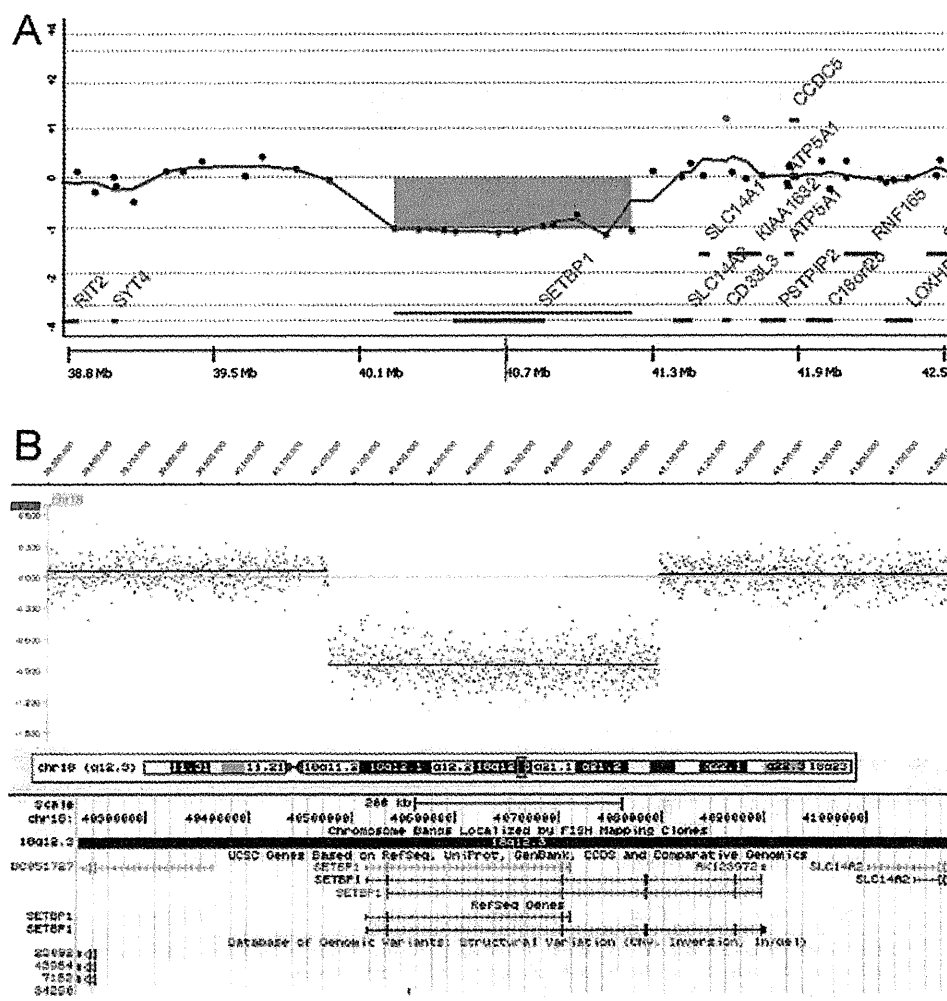

Figure 2 Microarray-based comparative genomic hybridisation identifies small deletions including *SETBP1* in patient 1 (A) and patient 2 (B). DNA copy number changes are represented by the negative $\log_2$ ratio below the baseline showing the deletions. (B) The square in the chromosome ideogram indicates the chromosomal position of the deletion; genes contained within the deletion are depicted below (http://genome.ucsc.edu).

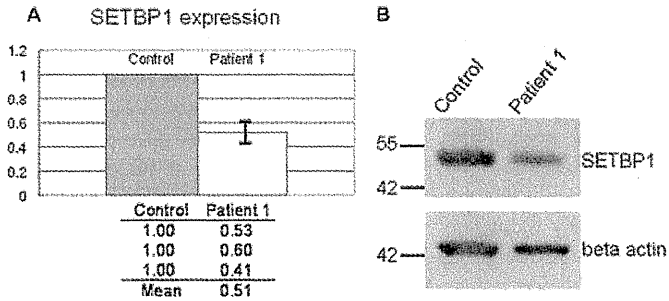

Figure 3 Expression studies. (A) SETBP1 RNA expression ratio analysed by real-time PCR. Raw data are given beneath the histogram. SETBP1 expression in the patient was about half that found in the control. (B) Western blotting of SETBP1. A total of 10 μg protein was separated in the gels. SETBP1 protein can be seen to be decreased in the patient. Beta actin was used as the internal control. Molecular mass (kDa) is indicated on the left of the gel.

protein concentration was also confirmed by western blotting (figure 3A,B).

Cohort study for *SETBP1* mutations

We identified 18 nucleotide changes including 11 non-synonymous and seven synonymous mutations, but no nonsense and no truncation mutations (table 1). The seven synonymous and four non-synonymous mutations, V231L, A390V, V1101I and P1130T, which were already listed in the single-nucleotide polymorphism database, were benign single-nucleotide polymorphisms. Four missense mutations (R627C, E958G, G1067S and W1242C; data not shown) located on the conserved sequence regions compared with the homologous genes from other species were not identified in normal control samples. However, W1242C was found in a healthy parent. Q1558L was also inherited from a healthy parent. The codon positions of E1466D and P1526Q were conserved among species and included in the important regions, SET-binging region and PPLPPPPP repeat, respectively. However, the patients' phenotypes were not similar to the presenting patient or SGS. Thus there was no definite pathogenic mutation. The sequence of the remaining *SETBP1* allele in patient 1 contained no nucleotide alterations.

DISCUSSION

In this study, we identified two patients with de novo chromosomal microdeletions in 18q12.3 that included *SETBP1* exclusively. *SETBP1* haploinsufficiency was suggested to be pathogenic. The patients exhibit moderate developmental delay and distinctive facial features, including prominent forehead, sparse eyebrows, mild ptosis with periorbital fullness. Patient 2 in particular showed a striking discrepancy between expressive speech impairment and conserved receptive speech, which has also been previously observed in patients with larger deletions in del(18)(q12.3q12.3). The complete and exclusive loss of one copy of *SETBP1* in our patient in correlation thus suggests an essential role for *SETBP1* in expressive speech development.

Schinzel *et al* reported on three patients with del(18)(q12.2q21.1) showing muscular hypotonia, seizures, behavioural disorders, and a pattern of minor dysmorphic features including prominent forehead, ptosis of the upper eyelids, full periorbital tissue, epicanthic folds and strabismus.[5] These phenotypic characteristics are similar to those in the cases presented here. Tinkle *et al* reported on a patient with del(18)(q12.2q21.1) with

Table 1 Identified nucleotide alteration in the cohort study

Nucleotide position*	Change	Amino acid change*	Location	Number of alleles that showed nucleotide changes	Conserved/ not conserved†	Function‡	Trio analyses	Results of population study	In silico database
c. 691	G>C	V231L	Exon 4	4	Not conserved				rs11082414
c. 1169	C>T	A390V	Exon 4	1	Not conserved				rs8091231
c. 1879	C>T	R627C	Exon 4	3	Conserved			None	None
c. 1911	G>A	P637P (synonymous)	Exon 4	1	-				None
c. 1932	C>T	S644S (synonymous)	Exon 4	2	-				rs3744824
c. 2607	C>T	S869S (synonymous)	Exon 4	12	-	The Ski homology region			None
c. 2873	A>G	E958G	Exon 4	1	Conserved			None	None
c. 3199	G>A	G1067S	Exon 4	1	Conserved			None	None
c. 3301	G>A	V1101I	Exon 4	90	Conserved				rs3744825
c. 3372	C>T	G1124G (synonymous)	Exon 4	1	-				None
c. 3388	C>A	P1130T	Exon 4	66	Conserved				rs1064204
c. 3726	G>C	W1242C	Exon 4	1	Conserved		Familial	None	None
c. 3825	A>G	S1275S (synonymous)	Exon 4	2	-				rs8096662
c. 4010	G>C	S1337S (synonymous)	Exon 5	1	-	SET-binding region			None
c. 4398	G>T	E1466D	Exon 6	3	Conserved	SET-binding region			None
c. 4563	C>G	P1521P (synonymous)	Exon 6	1	-	PPLPPPPP repeat			None
c. 4577	C>A	P1526Q	Exon 6	1	Conserved	PPLPPPPP repeat			None
c. 4673	A>T	Q1558L	Exon 6	1	Conserved		Familial		None

*Nucleotide and amino acid positions indicate NM_015559 sequence with the first initiation codon ATG at position 1.
†Conserved or not conserved was determined by comparison with the other species.
‡Functional domains were obtained from Minakuchi *et al* (2001).[12]

J Med Genet 2011;**48**:117–122. doi:10.1136/jmg.2010.084582

120

long-term survival, and concluded that life expectancy is minimally reduced.[6]

Although the previously reported chromosomal anomalies were identified at chromosomal G-banded levels, in more recent reports deletions in 18q12.2q21.1 were characterised by molecular techniques, and common features in the patients' phenotypes were reported.[7 8] The critical region for the phenotype of patients was narrowed to the 18q12.3-q21.1 region by Cody *et al*[9] and Buysse *et al*[10] (figure 4), who proposed a new syndrome involving expressive speech delay. They hypothesised that genes within the region may be specific to the neural and motor planning domains necessary for speech. However, deletions described so far contain numerous genes, including *SETBP1*, not allowing a phenotype–genotype correlation for haploinsufficiency of *SETBP1* exclusively.

Our findings correlate the phenotypes of the two patients with the exclusive complete loss of one copy of *SETBP1*. There is significant phenotypic overlap with the previously reported del (18)(q12.2q21.1) syndrome, suggesting a major contribution of the deletion of *SETBP1* to these phenotypes, as it has been described in contiguous deletion syndromes. The discrepancy between expressive and receptive language abilities in our patients appears to be a unique characteristic in the *SETBP1* deletion phenotype. The complete and exclusive loss of one copy of *SETBP1* in our patients in correlation with their phenotypes suggests an essential role for *SETBP1* in expressive speech development, although the exact function of the gene remains unknown.

SETBP1 encodes SET binding protein 1 expressed in numerous tissues including fetal brain. Its fusion with nucleoporin 98 kDa (*NUP98*) by chromosomal translocation has been shown in acute T-cell lymphoblastic leukaemia,[11] and the SET binding protein has been proposed to play a key role in the mechanism of SET-related leukaemogenesis and tumorigenesis by regulatory function in the nucleus.[12] Hoischen *et al* recently identified mutations in *SETBP1* to be causative of SGS, which is

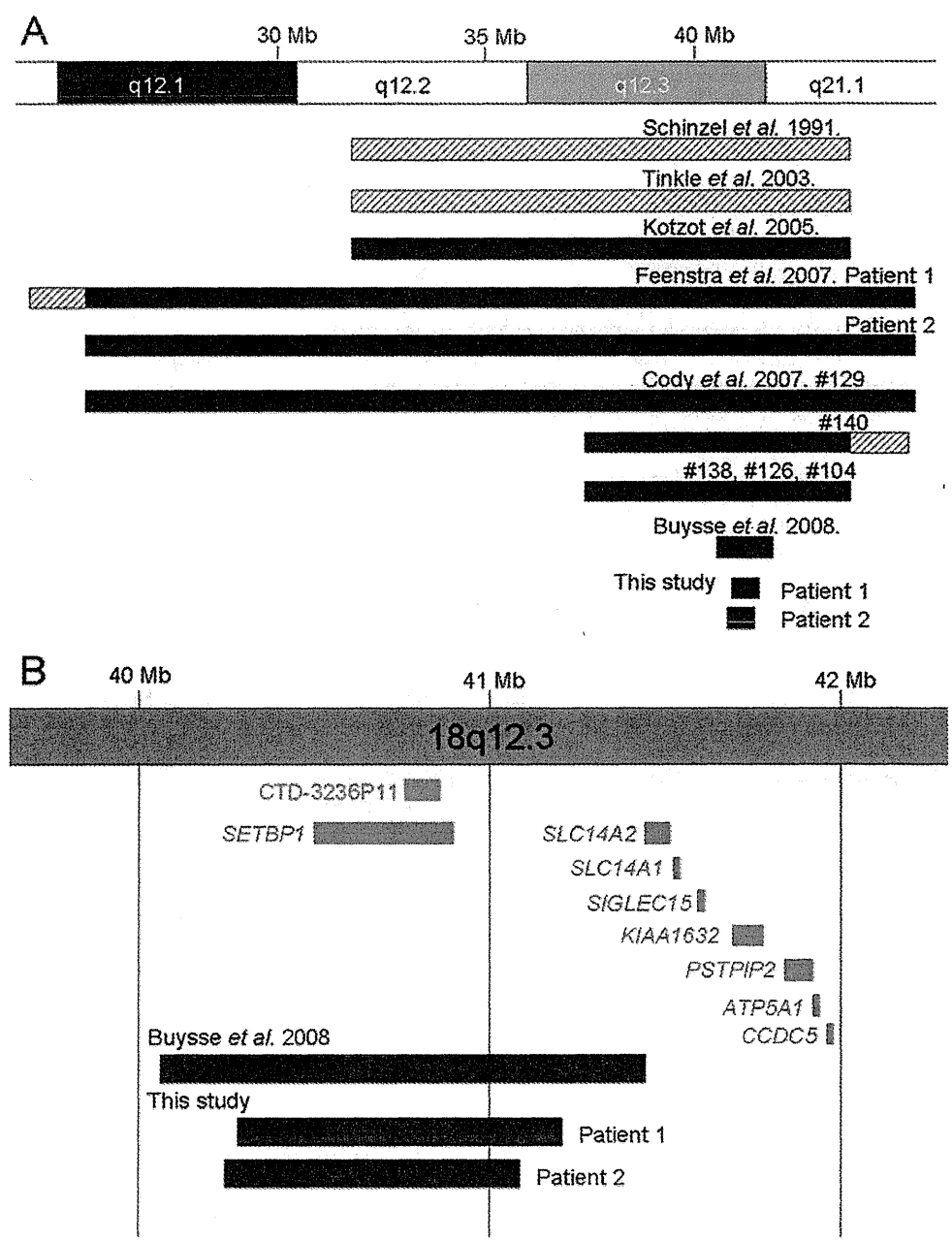

Figure 4 Comparison of the deletion regions. (A) Schematic representation of the previously reported deletions on a physical map of chromosome 18. (B) The deletion region of the patient is expanded. Bars filled with black and diagonal lines indicate definite and ambiguous deletion regions, respectively. Green and red bars indicate the position of the BAC clone used for fluorescence in situ hybridisation and the known genes, respectively.

characterised by severe mental retardation, distinctive facial features, and multiple congenital malformations.[1] Prognosis is poor, and most affected individuals die in the first decade of life. All reported mutations of *SETBP1* in patients with SGS were missense mutations in the important SET-binding region, and a gain-of-function or dominant-negative effect was suspected.[12]

As the phenotype of our two patients and the previously reported patients with del(18)(q12.2q21.1) including *SETBP1* does not resemble SGS and clinical features are generally milder, we conclude that haploinsufficiency of *SETBP1* does not cause SGS. We analysed the expression of SETBP1 by real-time PCR and western blotting, and found that SETBP1 was reduced in patient-derived skin fibroblasts, confirming that the effects of SETBP1 are allele dose-dependent. The deletion mainly affects speech, but the syndromic phenotype includes global development delay and recognisable facial dysmorphism underlying ubiquitous expression of SETBP1. As the phenotypic appearance of *SETBP1* haploinsufficiency is completely different from that of SGS, our findings support the proposed gain-of-function or dominant negative effect of the identified mutations in this gene.

There are various examples of phenotypic variability due to the different nature of mutations in the same gene. Mutations in fibroblast growth factor 3 (*FGFR3*) cause disproportionate growth in achondroplasia by gain-of-function, whereas terminal deletions of 4p including *FGFR3* cause Wolff–Hirschhorn syndrome, which does not show disproportionate growth at all, but small stature.[13 14] On the other hand, gain-of-function mutations of T-box 1 (*TBX1*) can result in the same phenotypic spectrum as haploinsufficiency caused by loss-of-function mutations or deletions in 22q11 including *TBX1*.[15]

In our study, we delimit a phenotype for haploinsufficiency of *SETBP1* distinct from the phenotype of SGS described in patients with mutations in the same gene suggesting a gain-of-function or a dominant negative effect of the mutations described. The *SETBP1* deletion phenotype seems to overlap extensively with the previously described del(18)(q12.2q21.1) syndrome, which has been characterised by moderate developmental delay, distinctive facial appearance, expressive language delay, and behavioural problems. Haploinsufficiency of *SETBP1* may thus primarily contribute to the phenotype of this contiguous gene syndrome. We did not identify pathogenic mutations on sequencing *SETBP1* in a cohort of 142 patients with developmental delay. Additional studies of the exact cellular function of *SETBP1* are needed to understand the pathogenic origin of the variable and distinct phenotypes.

Acknowledgements We thank the patients' parents for their gracious participation and support. We are grateful to the technicians from our laboratories, including Ms Etsuko Tanji, for their skilful help. We also acknowledge the DECIPHER database for comparing our data with those of others.

Funding This work was partially supported by a research grant from the University of Basel (DMS2058) and the Japan Ministry of Education, Science, Sports and Culture, Grant-in-Aid for Scientific Research (C), 21591334, 2010.

Competing interests None.

Patient consent Obtained.

Ethics approval This study was conducted with the approval of the Tokyo Women's Medical University and the University of Basel.

Provenance and peer review Not commissioned; externally peer reviewed.

REFERENCES

1. **Hoischen A,** van Bon BW, Gilissen C, Arts P, van Lier B, Steehouwer M, de Vries P, de Reuver R, Wieskamp N, Mortier G, Devriendt K, Amorim MZ, Revencu N, Kidd A, Barbosa M, Turner A, Smith J, Oley C, Henderson A, Hayes IM, Thompson EM, Brunner HG, de Vries BB, Veltman JA. De novo mutations of SETBP1 cause Schinzel-Giedion syndrome. *Nat Genet* 2010;**42**:483–5.
2. **Schefe JH,** Lehmann KE, Buschmann IR, Unger T, Funke-Kaiser H. Quantitative real-time RT-PCR data analysis: current concepts and the novel "gene expression's CT difference" formula. *J Mol Med* 2006;**84**:901–10.
3. **Shimojima K,** Komoike Y, Tohyama J, Takahashi S, Paez MT, Nakagawa E, Goto Y, Ohno K, Ohtsu M, Oguni H, Osawa M, Higashinakagawa T, Yamamoto T. TULIP1 (RALGAPA1) haploinsufficiency with brain development delay. *Genomics* 2009;**94**:414–22.
4. **Komoike Y,** Shimojima K, Liang JS, Fujii H, Maegaki Y, Osawa M, Fujii S, Higashinakagawa T, Yamamoto T. A functional analysis of GABARAP on 17p13.1 by knockdown zebrafish. *J Hum Genet* 2010;**55**:155–62.
5. **Schinzel A,** Binkert F, Lillington DM, Sands M, Stocks RJ, Lindenbaum RH, Matthews H, Sheridan H. Interstitial deletion of the long arm of chromosome 18, del (18)(q12.2q21.1): a report of three cases of an autosomal deletion with a mild phenotype. *J Med Genet* 1991;**28**:352–5.
6. **Tinkle BT,** Christianson CA, Schorry EK, Webb T, Hopkin RJ. Long-term survival in a patient with del(18)(q12.2q21.1). *Am J Med Genet A* 2003;**119A**:66–70.
7. **Kotzot D,** Haberlandt E, Fauth C, Baumgartner S, Scholl-Burgi S, Utermann G. Del (18)(q12.2q21.1) caused by a paternal sister chromatid rearrangement in a developmentally delayed girl. *Am J Med Genet A* 2005;**135**:304–7.
8. **Feenstra I,** Vissers LE, Orsel M, van Kessel AG, Brunner HG, Veltman JA, van Ravenswaaij-Arts CM. Genotype-phenotype mapping of chromosome 18q deletions by high-resolution array CGH: an update of the phenotypic map. *Am J Med Genet A* 2007;**143A**:1858–67.
9. **Cody JD,** Sebold C, Malik A, Heard P, Carter E, Crandall A, Soileau B, Semrud-Clikeman M, Cody CM, Hardies LJ, Li J, Lancaster J, Fox PT, Stratton RF, Perry B, Hale DE. Recurrent interstitial deletions of proximal 18q: a new syndrome involving expressive speech delay. *Am J Med Genet A* 2007;**143A**:1181–90.
10. **Buysse K,** Menten B, Oostra A, Tavernier S, Mortier GR, Speleman F. Delineation of a critical region on chromosome 18 for the del(18)(q12.2q21.1) syndrome. *Am J Med Genet A* 2008;**146A**:1330–4.
11. **Panagopoulos I,** Kerndrup G, Carlsen N, Strombeck B, Isaksson M, Johansson B. Fusion of NUP98 and the SET binding protein 1 (SETBP1) gene in a paediatric acute T cell lymphoblastic leukaemia with t(11;18)(p15;q12). *Br J Haematol* 2007;**136**:294–6.
12. **Minakuchi M,** Kakazu N, Gorrin-Rivas MJ, Abe T, Copeland TD, Ueda K, Adachi Y. Identification and characterization of SEB, a novel protein that binds to the acute undifferentiated leukemia-associated protein SET. *Eur J Biochem* 2001;**268**:1340–51.
13. **Richette P,** Bardin T, Stheneur C. Achondroplasia: from genotype to phenotype. *Joint Bone Spine* 2008;**75**:125–30.
14. **Altherr MR,** Wright TJ, Denison K, Perez-Castro AV, Johnson VP. Delimiting the Wolf-Hirschhorn syndrome critical region to 750 kilobase pairs. *Am J Med Genet* 1997;**71**:47–53.
15. **Zweier C,** Sticht H, Aydin-Yaylagul I, Campbell CE, Rauch A. Human TBX1 missense mutations cause gain of function resulting in the same phenotype as 22q11.2 deletions. *Am J Hum Genet* 2007;**80**:510–7.

Yasuda *et al. Molecular Autism* 2011, **2**:9
http://www.molecularautism.com/content/2/1/9

Molecular Autism

RESEARCH Open Access

Gene expression analysis in lymphoblasts derived from patients with autism spectrum disorder

Yuka Yasuda[1,2], Ryota Hashimoto[1,2,3*], Hidenaga Yamamori[1,4], Kazutaka Ohi[1,2], Motoyuki Fukumoto[1,2], Satomi Umeda-Yano[4], Ikuko Mohri[3,5], Akira Ito[4], Masako Taniike[3,5] and Masatoshi Takeda[1,3]

Abstract

Background: The autism spectrum disorders (ASDs) are complex neurodevelopmental disorders that result in severe and pervasive impairment in the development of reciprocal social interaction and verbal and nonverbal communication skills. In addition, individuals with ASD have stereotypical behavior, interests and activities. Rare mutations of some genes, such as neuroligin (*NLGN*) 3/4, neurexin (*NRXN*) 1, *SHANK3, MeCP2* and *NHE9*, have been reported to be associated with ASD. In the present study, we investigated whether alterations in mRNA expression levels of these genes could be found in lymphoblastoid cell lines derived from patients with ASD.

Methods: We measured mRNA expression levels of *NLGN3/4, NRXN1, SHANK3, MeCP2, NHE9* and *AKT1* in lymphoblastoid cells from 35 patients with ASD and 35 healthy controls, as well as from 45 patients with schizophrenia and 45 healthy controls, using real-time quantitative reverse transcriptase polymerase chain reaction assays.

Results: The mRNA expression levels of *NLGN3* and *SHANK3* normalized by *β-actin* or *TBP* were significantly decreased in the individuals with ASD compared to controls, whereas no difference was found in the mRNA expression level of *MeCP2, NHE9* or *AKT1*. However, normalized *NLGN3* and *SHANK3* gene expression levels were not altered in patients with schizophrenia, and expression levels of *NLGN4* and *NRXN1* mRNA were not quantitatively measurable in lymphoblastoid cells.

Conclusions: Our results provide evidence that the *NLGN3* and *SHANK3* genes may be differentially expressed in lymphoblastoid cell lines from individuals with ASD compared to those from controls. These findings suggest the possibility that decreased mRNA expression levels of these genes might be involved in the pathophysiology of ASD in a substantial population of ASD patients.

Background

Autism spectrum disorder (ASD), also known as pervasive developmental disorder (PDD), is defined as severe and pervasive impairments in the development of reciprocal social interaction and verbal and nonverbal communication skills. These disorders are also characterized by stereotypical behavior, interests and activities. The lifetime morbidity rate of ASD is 0.2% to 1.0% across studies [1]. In addition, twin and family studies of ASD have demonstrated a high heritability of approximately 90% [2], indicating that ASD is a heterogeneous condition that is likely to result from the combined effects of multiple genetic factors interacting with environmental factors. Recent genetic studies have identified several vulnerability loci and genetic mutations that cause ASD. One of the most striking revelations is the important role of genes that encode proteins at the neuronal synapse [3].

Rare mutations in the neuroligin 3 (*NLGN3*) and neuroligin 4 (*NLGN4*) genes, which map to chromosomes Xq13 and Xp22.3, have been reported in some patients with ASD and other neurodevelopmental impairments [4-8]. A particular mutation of *NLGN3* (Arg451Cys) is known to cause a defect in protein processing of *NLGN3* [9]. In addition, a particular mutation of *NLGN4* (1186insT) causes a frameshift mutation that leads to premature termination of *NLGN4* (D396X), resulting in a loss of 421 amino acids (51% of the

* Correspondence: hashimor@psy.med.osaka-u.ac.jp
[1]Department of Psychiatry, Osaka University Graduate School of Medicine, D3, 2-2, Yamadaoka, Suita, 565-0871, Osaka, Japan
Full list of author information is available at the end of the article

protein) [4]. Neuroligins, which are postsynaptically localized cell adhesion molecules, play a crucial role in organizing excitatory glutamatergic and inhibitory GABAergic synapses in the mammalian brain by interacting with presynaptic β-neurexins (*NRXN*), thereby triggering the formation of functional presynaptic structures in contacting axons [10]. Mutations of the neurexin 1 (*NRXN1*) gene, at the chromosome locus 2q32, have been found in individuals with ASD [11-14]. Furthermore, *de novo* copy number variation analysis revealed deletion of the *NRXN1*-containing gene region in ASD [15]. The binding of *NRXN1* and *NLGN* genes mediates synaptic development [16]. Interestingly, a mutation of *NLGN3* results in a disruption of the ability to bind to *NRXN* [9]. In addition, neuroligins interact with a postsynaptic scaffolding protein, SHANK3, which is also implicated in ASD [17] and is located on the telomeric terminal of chromosome 22q13.3. Shank proteins couple neurotransmitter receptors, ion channels and other membrane proteins to the actin cytoskeleton and G protein-coupled signaling pathways, and they also play a role in synapse formation and dendritic spine maturation [18]. Deletion or translocation of the genomic locus, which includes the *SHANK3* gene, and *de novo* mutations of the *SHANK3* gene result in premature stop codons and have been found in ASD [17,19,20].

In a study of consanguineous autism families, Morrow *et al.* [21] observed a relationship between ASD and alterations in the sodium/hydrogen exchanger 9 (*NHE9*) gene. Specifically, they found a nonsense mutation in patients with ASD that is a heterozygous CGA-to-TGA transition, changing arginine 423 to a stop codon [21]. The *NHE9* gene is located on chromosome 3q24 and is one of the families of Na^+/H^+ exchangers that regulate ion flux across membranes [22]. Rett syndrome is another PDD, and the methyl-CpG-binding protein 2 (*MeCP2*) gene is a causal gene for Rett syndrome. *MeCP2* is a transcriptional repressor that binds to methylated CpG dinucleotides generally located at gene promoters and recruits histone deacetylase 1 and other proteins involved in chromatin repression [23]. *De novo* mutations of the *MeCP2* gene located on chromosome Xp28 occur in 80% of female patients with Rett syndrome [24]. Some evidence of dysregulation of the phosphatidylinositol 3-kinase (PI3K)/AKT pathway is implicated in ASD, despite the fact that no mutation which causes ASD has been reported in association with the *AKT1* gene. The expression and phosphorylation and/or activation of AKT were found to be decreased in the autistic brain [25]. The *PTEN* gene (phosphatase and tensin homolog deleted on chromosome 10) is a major negative regulator of the PI3K/AKT pathway, and *PTEN* mutations have been linked to ASD [26].

Recently, several studies have suggested that lymphoblastoid cells can be used to detect biologically plausible correlations between candidate genes and neuropsychiatric diseases, including Rett syndrome [27], nonspecific X-linked mental retardation [28], bipolar disorder [29], fragile X syndrome [30,31] and dup(15q) [32]. In the present study, we compared mRNA expression levels of various genes in blood-derived lymphoblastoid cells from individuals with ASD and healthy controls.

Methods

Participants

We obtained mRNA samples from patients with ASD, patients with schizophrenia and healthy controls from the research bioresource of the Human Brain Phenotype Consortium in Japan (http://www.sp-web.sakura.ne.jp/consortium.html). The ASD cohort consisted of 35 patients with ASD and healthy controls (Table 1). Patients with ASD and patients with schizophrenia were recruited from both outpatient and inpatient services at Osaka University Hospital. Each ASD patient was diagnosed by at least two trained child psychiatrists and/or child neurologists according to the *Diagnostic and Statistical Manual of Mental Disorders, Fourth Edition-Text Revision* (DSM-IV-TR) criteria based on unstructured or semistructured behavioral observations of the patients and interviews with the patients and their parents or caregivers. During the interview, the Pervasive Developmental Disorders Autism Society Japan Rating Scale (PARS) [33] and the Japanese version of the Asperger's Questionnaire [34] were used to assist in the evaluation of ASD-specific behaviors and symptoms. PARS is a semistructured interview that is composed of

Table 1 Demographic information for the ASD and control cohorts[a]

Demographics	ASD (n = 35)	Controls (n = 35)	P value
Sex, M/F	27/8	26/9	χ^2 = 0.078 (1, N = 70), P = 0.78
Mean age, years (± SD)	12.9 (12.4)	34.8 (9.7)	U = 86, P = 0.60 × 10^{-9}, Z = -6.19
Age range, years	3 to 63	21 to 65	
Number of ASD (with IQ < 70)	35 (11)	0	
Number of Autism (with IQ < 70)	20 (10)	-	
Number of Asperger's syndrome (with IQ < 70)	11 (0)	-	
Number with PDD-NOS (with IQ < 70)	4 (1)	-	

ASD: autism spectrum disorder, M: male, F: female, IQ: intelligence quotient; PDD-NOS: pervasive developmental disorder not otherwise specified. Data are means ± SD unless otherwise specified. Differences in clinical characteristics were analyzed using the χ^2 test for gender and the Mann-Whitney U test for age.